JOURNAL OF GEOPHYSICAL RESEARCH, VOL. 97, NO. D16, PAGES 18,015–18,033, NOVEMBER 20, 1992

Impact of Heterogeneous Chemistry on Model Predictions of Ozone Changes

CLAIRE GRANIER AND GUY BRASSEUR

National Center for Atmospheric Research, Boulder, Colorado

A two-dimensional chemical/transport model of the middle atmosphere is used to assess the importance of chemical heterogeneous processes both in the polar regions (on polar stratospheric clouds (PSCs)) and at other latitudes (on sulfate aerosols). When conversion on type I and type II PSCs of N_2O_5 into HNO_3 and of $ClONO_2$ into reactive forms of chlorine is taken into account, enhanced ClO concentrations lead to the formation of a springtime "ozone hole" over the Antarctic continent. No such major reduction in the ozone column is found in the Arctic region. When conversion of nitrogen and chlorine compounds is assumed to occur on sulfate particles present in the lower stratosphere at all latitudes, significant perturbations in the chemistry are also found. For background aerosol conditions, the concentration of nitric acid is enhanced and agrees with observed values, while that of nitrogen oxides is reduced and agrees less than if heterogeneous processes are ignored in the model calculations. The concentration of the OH radical is significantly increased. Ozone number density appears to become larger between 16 and 30 km but smaller below 16 km, especially at high latitudes. The ozone column is only slightly modified, except at high latitudes where it is substantially reduced if the $ClONO_2$ conversion into reactive chlorine is taken into account. After a large volcanic eruption such as that of Mount Pinatubo in June 1991, these changes are further exacerbated. The ozone budget in the lower stratosphere becomes less affected by nitrogen oxides but is largely controlled by the ClO_x and HO_x chemistries. A substantial decrease in the ozone column is predicted as a result of the Pinatubo eruption, mostly in winter at midlatitudes and high latitudes. The predicted values depend on the assumption made for the evolution of the aerosol surface area density but is expected to be of the order of 10% at mid-latitudes in February and March 1992. An enhanced mixing ratio of ClO of the order of 100 parts per trillion by volume and a reduced mixing ratio of NO_2 below 25 km should be detected outside the polar vortex, especially in air masses with high levels of volcanic aerosols.

1. Introduction

Heterogeneous processes occurring on the surface of ice particles in polar stratospheric clouds are known to play a key role in the formation of the springtime ozone depletion in the Antarctic [*Solomon et al*, 1986; *McElroy et al.*, 1986]. These reactions lead to denitrification and dehydration of the lower polar stratosphere and convert chlorine reservoirs into active chlorine which destroys ozone in the presence of solar radiation. Heterogeneous processes are probably not limited to polar regions [*Hofmann and Solomon*, 1989; *Brasseur et al.*, 1990*b*]. The natural background aerosol, mainly composed of sulfuric acid and water is present throughout the lower stratosphere [*Junge*, 1961]. Its origin is related to direct injection of sulfuric acid by volcanic eruptions and to oxidation of sulfur-containing gases. Aerosol particles provide surfaces on which reactions similar to those occurring on the PSC particles surfaces may occur [*Tolbert et al.*, 1988*a*; *Worsnop et al.*, 1988]. The aerosol particles in the Junge layer are much smaller (radius of 0.05–0.2 μm) than the polar stratospheric clouds particles (1–100 μm); they provide less surface area available for heterogeneous reactions to occur. Thus, the effects of these reactions are expected to be smaller than in the polar regions. However, large amounts of sulfuric acid particles are occasionally injected into the stratosphere as a result of volcanic eruptions, with potential effects on the ozone layer. Measurements performed in the northern mid-latitudes [*Bais et al.*, 1985; *Mantis et al.*, 1986; *Dütsch*, 1985] suggest that ozone did decrease in late 1982 and in 1983, following the eruption of El Chichón, in Mexico [*Hofmann and Solomon*, 1989], although the quasi-biennial oscillation in the circulation of the atmosphere might also have contributed to the observed signal in the ozone column during this period [*Chandra and Stolarski*, 1991]. The more recent eruption of Mount Pinatubo in the Philippines (June 1991) has injected in the stratosphere approximately twice as much sulfur as El Chichón [*McCormick and Veiga*, 1992], creating the potential for large ozone depletion [*Brasseur et al.*, 1990*b*; *Brasseur*, 1991; *Prather*, 1992; *Bekki and Pyle*, 1992].

The purpose of this paper is to study the potential effects of heterogeneous processes on the global ozone budget in the stratosphere and to determine how these reactions, which were ignored in most earlier model simulations, could affect the predictions of future ozone changes resulting from increasing levels of anthropogenic chlorine in the atmosphere. The model used in this work is described in section 2, while the parameterizations of the heterogeneous processes in polar stratospheric clouds and sulfate aerosols are detailed in section 3. The results of the simulations for the polar regions are discussed in section 4, and evaluations of the effects of the stratospheric sulfate aerosols on the stratosphere are given in section 5. Finally, an analysis of the past evolution of stratospheric ozone is presented in section 6.

Paper number 92JDO2021.
0148-0227/92/92JD-02021 $05.00

2. The Two-Dimensional Model

The model used to assess the importance of heterogeneous reactions in the atmosphere is two dimensional and extends

from the surface to 85 km, with a vertical resolution of 1 km, and from 85°S to 85°N with a latitudinal resolution of 5 degrees. As described by *Brasseur et al.* [1990*a*], radiation, chemistry and dynamics are treated interactively only above 15 km altitude. The formulation of the transport equations is based on the transformed Eulerian mean meridional circulation [*Andrews and McIntyre*, 1976], and a parameterization of the effects of the Rossby and gravity waves is included [*Brasseur and Hitchman*, 1987; *Hitchman and Brasseur*, 1988]. The net diabatic heating rate is calculated by using the radiative code of the National Center for Atmospheric Research Community Climate Model [*Kiehl et al.*, 1987] below 60 km. Above this altitude a Newtonian cooling formulation is used. Radiative effects of the stratospheric aerosol layer, however, are not taken into account.

The latest version of the model includes 55 species. The concentrations of the following chemical compounds (CO, CO_2, N_2O, HNO_3, N_2O_5, H, HF, H_2O, H_2, H_2O_2, CH_4, HCN, CH_3CN, CCl_4, $CFCl_3$, CF_2Cl_2, CH_3CCl_3, CH_3Cl, CFC-113, HCFC-22, Halon-1211, Halon-1301, CFC-114, CFC-115, CCl_2O, CClFO, CF_2O, CH_3Br, OCS, SO_2, H_2SO_4) are calculated by solving for each of them a full continuity/transport equation. Short-lived species are grouped into long-lived families ($O_x = O + O_3 + O^1D$, $NO_y = N + NO + NO_2 + NO_3 + HO_2NO_2 + ClONO_2 + HNO_3 + 2\,N_2O_5$, $Cl_x = Cl + ClO + HOCl + HCl + ClONO_2 + OClO + 2\,Cl_2O_2$, $Br_x = Br + BrO + BrONO_2 + HBr + HOBr$), for which a continuity/transport equation is solved. The concentration of each individual fast reacting species is then derived by assuming photochemical equilibrium conditions for the fastest reacting species and by a time integration for the other compounds. Instantaneous photochemical equilibrium conditions are assumed for the species belonging to the HO_x family. The rate of the reactions included in the model, given in Tables 1*a*, 1*b*, and 1*c*, are based on the Jet Propulsion Laboratory 1990 compilation [*DeMore et al.*, 1990]. The photodissociation rates are calculated from the solar irradiances given by *Brasseur and Simon* [1981] and the absorption cross-sections compiled by *De More et al.* [1990]. The absorption cross-sections of the chlorofluorocarbons as a function of temperature are taken from *Simon et al.* [1988]. The model is integrated using an alternating direction implicit method with a time step of 15 days.

3. Parameterizations of the Heterogeneous Chemical Processes

3.1. Polar Stratospheric Clouds

In the presence of polar stratospheric clouds (PSCs) at high latitudes, chlorine reservoir species are converted into more reactive chlorine, and nitrogen oxides are transformed into nitric acid. The main heterogeneous reactions involved are believed to be [*Molina et al.*, 1987; *Leu*, 1988; *Tolbert et al.*, 1988*b*, *Hanson and Ravishankara*, 1991]

$$ClONO_2\,(g) + H_2O\,(s) \rightarrow HOCl\,(g) + HNO_3\,(s)$$

$$HOCl\,(g) + HCl\,(s) \rightarrow Cl_2\,(g) + H_2O\,(s)$$

$$ClONO_2\,(g) + HCl\,(s) \rightarrow Cl_2\,(g) + HNO_3\,(s)$$

$$N_2O_5\,(g) + H_2O\,(s) \rightarrow 2\,HNO_3\,(s)$$

$$N_2O_5\,(g) + HCl\,(s) \rightarrow ClNO_2\,(g) + HNO_3\,(s)$$

where (g) indicates that the molecule is produced in the gas phase and (s) indicates a solid solution.

Polar stratospheric clouds are observed during winter and early spring in the Antarctic between 12 and 24 km altitude [*McCormick et al.*, 1982] and in the Arctic at somewhat higher altitudes [*World Meteorological Organization (WMO)*, 1990]. Two major types of polar stratospheric clouds have been identified in Antarctica [*Toon et al.*, 1989; *Turco et al.*, 1989]: The type II PSCs, mainly composed of water ice with traces of nitric acid, are formed in regions where the temperature is lower than 187 K [*Turco et al.*, 1989]. These particles are relatively large (10–100 μm) and therefore provide a way to remove water and nitric acid from the atmosphere by sedimentation, at a rate of several kilometers per week [*Turco et al.*, 1989]. The type I PSCs appear to be mainly composed of nitric acid trihydrate and are formed at temperatures below 195 K [*Turco et al.*, 1989]; these particles are small (0.1–1 μm), and very little sedimentation is expected. They are observed both in the Arctic and the Antarctic.

TABLE 1*a*. Chemical Reactions Included in the Model and Corresponding Rate Constants ($cm^3\ s^{-1}$)

Chemical Reaction	Rate Constant
$O + O + M \rightarrow O_2 + M$	4.3E-28 $(T)^{-2}$ [M]
$O + O_2 + M \rightarrow O_3 + M$	6.0E-34 $(300/T)^{2.3}$[M]
$O + O_3 \rightarrow O_2 + O_2$	8.0E-12 exp(-2060/T)
$O(^1D) + N_2 \rightarrow O + N_2$	1.8E-11 exp(110/T)
$O(^1D) + O_2 \rightarrow O + O_2$	3.2E-11 exp(70/T)
$O(^1D) + H_2O \rightarrow OH + OH$	2.2E-10
$H + O_3 \rightarrow O_2 + OH$	1.4E-10 exp(-470/T)
$O(^1D) + CH_4 \rightarrow CH_3 + OH$	1.4E-10
$O(^1D) + H_2 \rightarrow OH + H$	1.0E-10
$O + OH \rightarrow O_2 + H$	2.2E-11 exp(120/T)
$OH + O_3 \rightarrow HO_2 + O_2$	1.6E-12 exp(-940/T)
$HO_2 + O_3 \rightarrow OH + 2O_2$	1.1E-14 exp(-500/T)
$O + HO_2 \rightarrow OH + O_2$	3.0E-11 exp(200/T)
$OH + HO_2 \rightarrow H_2O + O_2$	4.8E-11 exp(250/T)

Chemical Reaction	Rate Constant
$OH + H_2 \rightarrow H_2O + H$	5.5E-12 exp(-2000/T)
$H + HO_2 \rightarrow OH + OH$	7.3E-11
$H + HO_2 \rightarrow H_2 + O_2$	6.5E-12
$H + HO_2 \rightarrow H_2O + O$	1.6E-12
$H_2 + O \rightarrow OH + H$	8.8E-12 exp(-4200/T)
$HO_2 + HO_2 \rightarrow H_2O_2 + OH$	2.3E-13 exp(600/T)
$H_2O_2 + OH \rightarrow H_2O + HO_2$	2.9E-12 exp(-160/T)
$NO + HO_2 \rightarrow NO_2 + OH$	3.7E-12 exp(240/T)
$OH + CO \rightarrow CO_2 + H$	1.35E-13 (1 + 0.6 P_{atm})
$O + NO_2 \rightarrow NO + O_2$	6.5E-12 exp(120/T)
$O_3 + NO \rightarrow NO_2 + O_2$	2.0E-12 exp(-1400/T)
$N + NO \rightarrow N_2 + O$	3.4E-11
$N + O_2 \rightarrow NO + O$	1.5E-11 exp(-3600/T)
$O_3 + NO_2 \rightarrow NO_3 + O_2$	1.2E-13 exp(-2450/T)
$HNO_3 + OH \rightarrow H_2O + NO_3$	9.4E-15 exp(778/T)
$HO_2NO_2 + OH \rightarrow H_2O + NO_2 + O_2$	1.3E-12 exp(380/T)
$N_2O + O(^1D) \rightarrow N_2 + O_2$	4.9E-11
$N_2O + O(^1D) \rightarrow NO + NO$	6.7E-11
$CH_4 + OH \rightarrow CH_3 + H_2O$	2.9E-12 exp(-1815/T)
$CH_3O_2 + NO \rightarrow CH_3O + NO_2$	4.2E-12 exp(180/T)
$CH_2O + OH \rightarrow HCO + H_2O$	1.1E-11
$CH_2O + O \rightarrow CHO + OH$	3.4E-11 exp(-1600/T)
$CH_3O_2 + CH_3O_2 \rightarrow$ products	2.2E-13 exp(220/T)
$OH + CH_3CN \rightarrow$ products	5.9E-13 exp (-750/T)
$CH_3CN + Cl \rightarrow$ products	8.0E-11 exp(-3000/T)
$O(^1D) + CH_3CN \rightarrow$ products	1.0E-10
$O(^1D) + HCN \rightarrow$ products	1.0E-10
$CH_3Cl + OH \rightarrow CH_2Cl + H_2O$	2.1E-12 exp(-1150/T)
$Cl + O_3 \rightarrow ClO + O_2$	2.9E-11 exp(-260/T)
$ClO + O \rightarrow Cl + O_2$	3.0E-11 exp(70/T)
$ClO + NO \rightarrow Cl + NO_2$	6.4E-12 exp(290/T)
$Cl + CH_4 \rightarrow HCl + CH_3$	1.1E-11 exp(-2300/T)
$Cl + HO_2 \rightarrow HCl + O_2$	1.8E-11 exp(170/T)
$Cl + H_2 \rightarrow HCl + H$	3.7E-11 exp(-2300/T)
$Cl + CH_2O \rightarrow HCl + HCO$	8.1E-11 exp(-30/T)
$OH + HCl \rightarrow H_2O + Cl$	2.6E-12 exp(-350/T)
$ClONO_2 + O \rightarrow ClO + NO_3$	2.9E-12 exp(-800/T)
$ClO + HO_2 \rightarrow HOCl + O_2$	4.8E-13 exp(700/T)
$HOCl + O \rightarrow ClO + OH$	1.0E-11 exp(-2200/T)
$HOCl + OH \rightarrow H_2O + ClO$	3.0E-12 exp(-500/T)
$OClO + OH \rightarrow HOCl + O_2$	4.5E-13 exp(800/T)
$OClO + Cl \rightarrow ClO + ClO$	3.4E-11 exp(160/T)
$OClO + O \rightarrow ClO + O_2$	2.8E-11 exp(-1200/T)
$OClO + NO \rightarrow ClO + NO_2$	2.5E-12 exp(-600/T)
$CH_3CCl_3 + OH \rightarrow CH_2CCl_3 + H_2O$	5.0E-12 exp(-1800/T)
HCFC-22 + OH → Cl + products	1.2E-12 exp(-1650/T)
$Br + O_3 \rightarrow BrO + O_2$	1.7E-11 exp(-850/T)
$BrO + O \rightarrow Br + O_2$	3.0E-11
$BrO + NO \rightarrow Br + NO_2$	8.8E-12 exp(260/T)
$BrO + ClO \rightarrow Br + OClO$	6.7E-12
$BrO + ClO \rightarrow Br + Cl + O_2$	2.9E-12 exp (220/T) + 5.8E-13 exp(170/T)
$BrO + BrO \rightarrow Br + Br + O_2$	1.4E-12 exp(150/T)
$Br + HO_2 \rightarrow HBr + O_2$	1.5E-11 exp(-600/T)
$Br + OClO \rightarrow BrO + ClO$	2.6E-11 exp(-1300/T)

Here 4.3E-28 corresponds to 4.3×10^{-28}. T is the temperature (K), [M] is the atmospheric density (cm^{-3}), and P_{atm} is the pressure expressed in atmosphere.

TABLE 1*b*. Three-body Reaction With Rate Constant k ($cm^3\ s^{-1}$)

$$k=[\kappa_0[M]/(1+\kappa_0[M]/\kappa_\infty)]\times 0.6^{(1+[\log_{10}(\kappa_0[M]/\kappa_\infty)]^2)^{-1}}$$

Reaction	Rate Constant	Exponent
$NO_3 + NO_2 + M \rightarrow N_2O_5 + M$	κ_0^{300} = 2.2E-30	n = 4.3
	κ_∞^{300} = 1.5E-12	m = 0.5
	k_{eq} = 4E-27 exp(10930/T)	
$NO_2 + OH + M \rightarrow HNO_3 + M$	κ_0^{300} = 2.6E-30	n = 3.2
	κ_∞^{300} = 2.4E-11	m = 1.3
$NO_2 + HO_2 + M \rightarrow HO_2NO_2 + M$	κ_0^{300} = 1.8E-31	n = 3.2
	κ_∞^{300} = 4.7E-12	m = 1.4
	k_{eq} = 2.1E-27 exp(10900/T)	
$ClO + NO_2 + M \rightarrow ClONO_2 + M$	κ_0^{300} = 1.8E-31	n = 3.4
	κ_0^{300} = 1.5E-11	m = 1.9
$H + O_2 + M \rightarrow HO_2 + M$	κ_0^{300} = 5.7E-32	n = 1.6
	κ_∞^{300} = 7.5E-11	m = 0.0
$ClO + ClO + M \rightarrow Cl_2O_2 + M$	κ_0^{300} = 1.8E-32	n = 3.6
	κ_∞^{300} = 6.0E-12	m = 0.0
	k_{eq} = 3 E-27 exp(8450/T)	
$BrO + NO_2 + M \rightarrow BrONO_2 + M$	κ_0^{300} = 5.2E-31	n = 3.8
	κ_∞^{300} = 9.0E-12	m = 2.3

$\kappa = \kappa_0^{300}(T/300)^{-n}$ and $\kappa_\infty = \kappa_\infty^{300}(T/300)^{-m}$. The equilibrium constants k_{eq} (cm^3) for the reactions which form products thermally unstable at atmospheric temperatures are also indicated.

In the model, the type I PSCs are assumed to be formed in less than a time step (15 days) as soon as the temperature decreases below 197 K. Similarly, type II PSCs are assumed to be present in the regions where the temperature drops below 191 K. These temperature thresholds are a few degrees higher than the thermodynamical ones [*Turco et al.*, 1989]. This choice has been made to account for the fact that the temperatures calculated by the two-dimensional model correspond to zonal averages, which are somewhat higher than those of the coldest air masses in which polar air is processed. The conversion of HCl and $ClONO_2$ into chlorine radicals is assumed to take place in less than a model time step. In regions where PSC type II particles are present, dehydration and denitrification by heterogeneous reactions in the lower stratosphere are assumed to occur with an effective time constant of 5 days. In the region where PSC type I particles are present, no dehydration takes place, but a weak denitrification is assumed to occur, with an effective time constant of 30 days.

When the sun returns over the polar regions after the winter season, in addition to the classic catalytical cycles destroying odd oxygen in the background atmosphere [*Solomon et al.*, 1986; *Brasseur and Solomon*, 1986], ozone is also destroyed through different catalytical cycles involving the Cl_2O_2 dimer [*Molina and Molina*, 1987] and by an additional cycle requiring the presence of bromine oxide BrO [*McElroy et al.*, 1986].

3.2. Stratospheric Sulfate Aerosol Layer

Laboratory work [*Worsnop et al.*, 1988; *Mozurkewich and Calvert*, 1988; *Tolbert et al.*, 1988*a*; *Fried et al.*, manuscript in preparation, 1992] has shown that heterogeneous reactions similar to the ones occurring on the PSCs particles could also occur on the sulfate aerosol surfaces. As the solubility of HCl in the aerosol is expected to be considerably less than in ice [*Hanson and Ravishankara*, 1991], only the reactions with H_2O have to be considered. Furthermore, it is assumed that nitric acid resulting from these reactions is released into the gas phase. Thus, the reactions are

$$ClONO_2 + H_2O \text{ (sulfate aerosol)} \rightarrow HOCl\ (g) + HNO_3\ (g) \quad (1)$$

$$N_2O_5\ (g) + H_2O \text{ (sulfate aerosol)} \rightarrow 2\ HNO_3\ (g) \quad (2)$$

The first-order rate constant k for a reaction between a molecule and an aerosol particle can be written as [*Cadle et al.*, 1975] $k = \gamma v A/4$, where γ is the reaction probability, that is, the probability that a collision between a gas molecule and a particle results in a chemical reaction. The mean molecular speed v is given by $v = (8\ kT/\pi M)^{1/2}$, T is the atmospheric temperature, and M is the molecular mass. The total aerosol surface area density A corresponds to the total aerosol surface per unit volume unit available for heterogeneous reactions and is given by

$$A = \int_o^\infty 4\pi r^2 n(r)\,dr$$

where n(r) ($cm^{-3}\ \mu m^{-1}$) is the differential aerosol size distribution at radius r.

Reaction probabilities for heterogeneous reactions on sulfate aerosols as a function of temperature and aerosol composition have been measured recently by *Tolbert et al.* [1988*a*] , M. A. Tolbert (private communication, 1991), and *Hanson and Ravishankara* [1991] in the case of reaction (1), and by *Mozurkewich and Calvert* [1988], *Fried et al.*[1991], *Worsnop et al.* [1988] and *Hanson and Ravishankara* [1991] in the case of reaction (2). The experimental values of these reaction probabilities are shown on Figure 1 as a function of the aerosol composition, that is, the weight percentage of sulfuric acid in the particles. The measurements of the reaction

TABLE 1c. The Photochemical Reactions Included in the Model

	Reaction
$J(O_2)$	$O_2 + h\nu \rightarrow O(^3P) + O(^3P)$
$J^*(O_2)$	$O_2 + h\nu \rightarrow O(^1D) + O(^3P)$
$J(O_3)$	$O_3 + h\nu \rightarrow O(^3P) + O_2$
$J^*(O_3)$	$O_3 + h\nu \rightarrow O(^1D) + O_2$
$J(H_2O)$	$H_2O + h\nu \rightarrow OH + H$
$J(N_2O)$	$N_2O + h\nu \rightarrow N_2 + O(^1D)$
$J(CO_2)$	$CO_2 + h\nu \rightarrow CO + O$
$J(CH_4)$	$CH_4 + h\nu \rightarrow$ products
J(NO)	$NO + h\nu \rightarrow N + O$
$J(NO_2)$	$NO_2 + h\nu \rightarrow NO + O(^3P)$
$J(HNO_3)$	$HNO_3 + h\nu \rightarrow NO_2 + OH$
$J(CF_2Cl_2)$	$CF_2Cl_2 + h\nu \rightarrow CF_2Cl + Cl$
$J(CFCl_3)$	$CFCl_3 + h\nu \rightarrow CFCl_2 + Cl$
$J(CCl_4)$	$CCl_4 + h\nu \rightarrow CCl_3 + Cl$
J(HCl)	$HCl + h\nu \rightarrow H + Cl$
J(HOCl)	$HOCl + h\nu \rightarrow OH + Cl$
$J(CH_3CCl_3)$	$CH_3CCl_3 + h\nu \rightarrow CH_3CCl_2 + Cl$
$J(HO_2NO_2)$	$HO_2NO_2 + h\nu \rightarrow NO_2 + HO_2$
$J(CH_3Cl)$	$CH_3Cl + h\nu \rightarrow CH_3 + Cl$
$J(ClONO_2)$	$ClONO_2 + h\nu \rightarrow NO_3 + Cl$
J(OClO)	$OClO + h\nu \rightarrow O + ClO$
$J(Cl_2O_2)$	$Cl_2O_2 + h\nu \rightarrow Cl + ClOO$
$J(CCl_2O)$	$CCl_2O + h\nu \rightarrow$ products
J(CClFO)	$CClFO + h\nu \rightarrow$ products
$J(CF_2O)$	$CF_2O + h\nu \rightarrow$ products
$J(N_2O_5)$	$N_2O_5 + h\nu \rightarrow NO_2 + NO_3$
$J(H_2O_2)$	$H_2O_2 + h\nu \rightarrow OH + OH$
$J(H_2CO)$	$H_2CO + h\nu \rightarrow HCO + H$
$J(BrONO_2)$	$BrONO_2 + h\nu \rightarrow BrO + NO_2$
$J^*(BrONO_2)$	$BrONO_2 + h\nu \rightarrow Br + NO_3$
J(HOBr)	$HOBr + h\nu \rightarrow Br + OH$
$J(CH_3Br)$	$CH_3Br + h\nu \rightarrow Br +$ products
J(CFC-113)	CFC-113 + hν → 3 Cl + products
J(CFC-114	CFC-114 + hν → 2 Cl + products
J(CFC-115)	CFC-115 + hν → Cl + products
J(CFC-22)	CFC-22 + hν → Cl + products
J(H-1211)	H-1211 + hν → Cl + Br + products
J(H-1301)	H-1301 + hν → Br + products

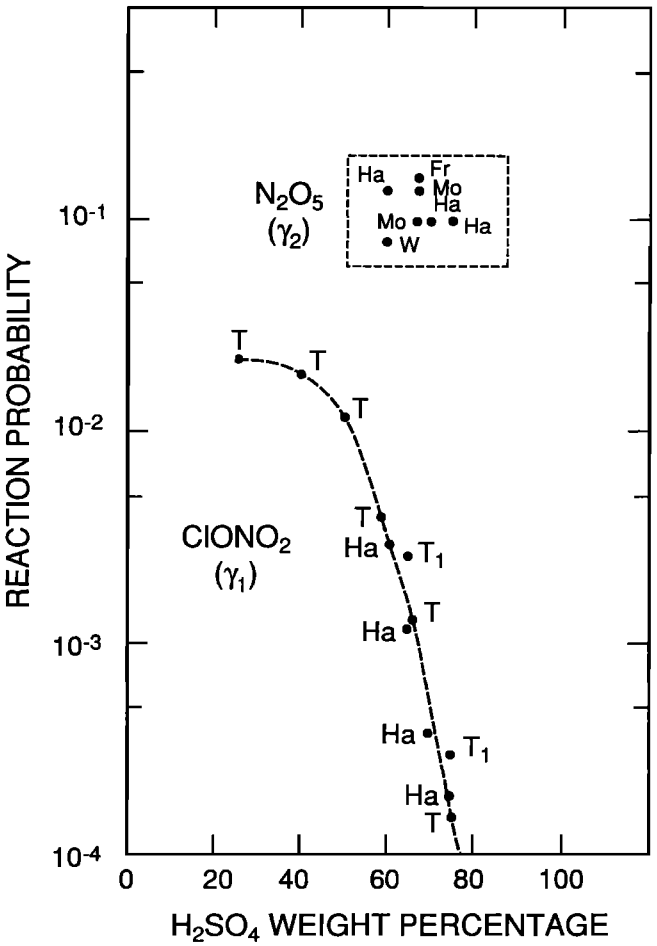

Fig. 1. Reaction probability of the $ClONO_2$ and N_2O_5 heterogeneous conversion on the surface of sulfate aerosol particles. Values determined by several authors are expressed as a function of the H_2SO_4 weight percentage in aerosol droplets. T, M. A. Tolbert (private communication, 1991); T1, *Tolbert et al.* [1988*a*]; Ha, *Hanson and Ravishankara* [1991]; Fr, *Fried et al.* (manuscript in preparation, 1992); Mo, *Mozurkewich and Calvert* [1988]; W, *Worsnop et al.* [1988].

probability for reaction (1) by M. A. Tolbert (private communication, 1991), made at 223 K, give values comparable to those by *Hanson and Ravishankara* [1991], performed in the 215–250 K temperature range, for a 60 to 75% H_2SO_4 solution. In the model simulations, the values suggested by M. A. Tolbert (private communication, 1991) as a function of the aerosol composition are used.

Measurements made by *Hanson and Ravishankara* [1991] for reaction (2) at stratospheric temperatures provide reaction probabilities close to the one determined at room temperature (between 0.1 and 0.14, see *Mozurkewich and Calvert* [1988]) and those measured by A. Fried et al. (manuscript in preparation, 1992) (between 0.095 and 0.15 at temperatures between 273 and 230 K). No systematic variation of this reaction probability with aerosol composition can be deduced from the current available measurements. In the simulations, a working value of 0.14, independent of the aerosol composition, has been used.

The stratospheric layer, discovered 30 years ago [*Junge et al.*, 1961] extends from the tropopause to about 25-30 km. The composition, size distribution, and radiative properties of these particles have been established through a large number of observations [*McCormick et al.*, 1979; *Hofmann and Rosen*, 1984*b*; *Turco et al.*, 1982]. During nonvolcanic periods, this sulfate layer is believed to be produced by photochemical and microphysical processes involving the photolysis of carbonyl sulfide [*Crutzen*, 1976]. The sulfur atoms produced are oxidized into sulfuric acid (H_2SO_4), which subsequently condense into submicron droplets. During volcanic eruptions, large amounts of sulfur are injected into the atmosphere, producing eventually a large increase in the aerosol load of the stratosphere.

The aerosol composition, that is, the H_2SO_4 weight percentage in the aerosols (60% to 80% [see *Rosen*, 1971; *Hofmann and Rosen*, 1984*a*]) depends mainly on the background temperature and water vapor mixing ratio. A detailed study of the equilibrium composition of sulfuric acid—water solution droplets has been conducted by *Steele and Hamill* [1981]. These theoretical evaluations have been shown to be in a good agreement with balloon measurements of the aerosol composition [*Hofmann and Solomon*, 1989]. In the model calculations, the reaction probability of reaction (1) has been derived, based on the H_2SO_4 weight percentage calculated

as a function of the calculated temperature and water vapor mixing ratios, based on *Steele and Hamill* [1981].

The total aerosol surface area density (A) in the stratosphere is variable by several orders of magnitude as a function of time. Systematic measurements of the aerosol distributions began in the early 1970s, and since this period, large amounts of volcanic matter have been injected into the stratosphere during at least six eruptions (Fuego, 1974; St. Helens, 1980; Alaid, 1981; El Chichón, 1982; Nevado del Ruiz, 1985; Pinatubo, 1991). The lowest aerosol densities for the last 3 decades have been found during the 1974 and 1978–1979 periods; this situation will be referred to as a background period. A high aerosol load has been observed in late 1982 to early 1983, after the El Chichón eruption, which affected mainly the northern hemisphere. Since this very large eruption, the aerosol load in the stratosphere has continuously declined but has increased again in 1991 after the eruption of Pinatubo. It is believed that this late volcano has injected approximately 19 Mt [*Bernard et al.*, 1991] of sulfur in the stratosphere, that is, 3 times more than El Chichón.

The distribution of the aerosol surface area adopted for background conditions is based on vertical profiles determined by *Hofmann* [1987] from balloon-borne measurements. Figure 2 [see *Hofmann and Solomon,* 1989] presents such a profile measured during September 1979 in Laramie, Wyoming (41°N). The stratospheric aerosol layer extends up to 26 km, with a maximum surface area density of 0.7 μm^2 cm^{-3} around 20 km altitude. Data displayed by *Rosen et al.* [1975] and by *Turco et al.* [1982] show that the aerosol layer appears to be relatively well mixed over the northern hemisphere, with a maximum aerosol mixing ratio located 6 to 8 km above the tropopause level. In the simulations, the latitudinal distribution of the aerosol surface area has been established by assuming that the distance between the tropopause level and the altitude of the maximum surface area is constant with latitude. This has been achieved through a translation of the surface area profile observed at 41°N and shown in Figure 2. This distribution is assumed to remain constant over the entire model integrations dealing with background conditions. It should be noted that measurements by *Hofmann* [1990] suggest that since 1974, the aerosol mass mixing ratio of the largest particles (radius greater than 0.25 μm) during the background situations has increased by about 5% per year, while no significant change is reported for the smallest particles.

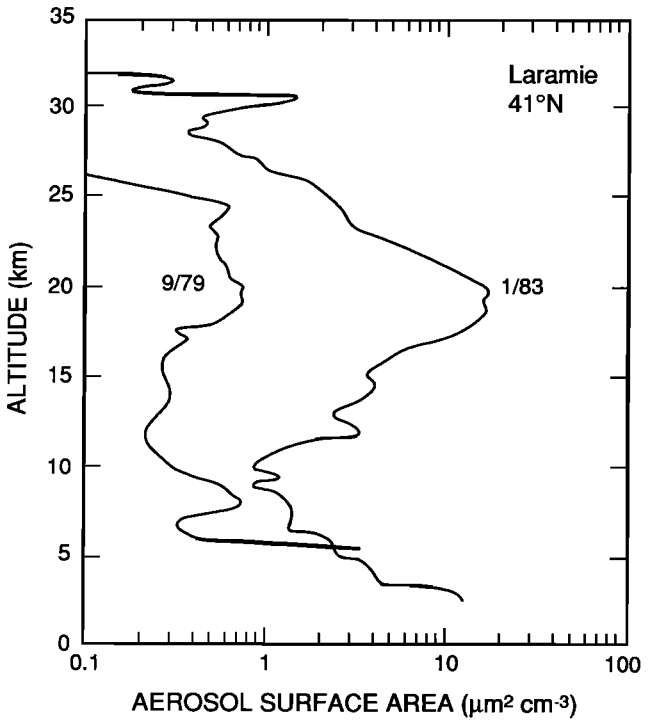

Fig. 2. Total aerosol surface area density measured at Laramie (41°N) in September 1979 (background conditions) and January 1983 (postvolcanic conditions) [from *Hofmann and Solomon*, 1989].

4. Model Simulations in the Polar Regions

4.1. The Polar Regions

Before performing model predictions of future ozone changes, it is appropriate to validate the parameterizations described earlier by simulating the present distribution and past evolution of the ozone and other chemical compounds abundance. In a first part of the discussion, the only heterogeneous processes included in the model will be those occurring on the surface of particles in polar stratospheric clouds. The assumed history of trace gas concentrations is presented in Table 2, similar to scenario A used in the recent WMO/United Nations Environment Program Scientific Assessment of Stratospheric Ozone [*WMO*, 1990].

Figure 3*a* shows the variation as a function of latitude and season of the ozone column abundance calculated at steady state for 1970 conditions (level of active chlorine is 1.55 parts per billion by volume (ppbv)). The model reproduces the well-established features in the ozone distribution: The column abundance increases with latitude from about 260 Dobson at the equator to 480 Dobson at the North Pole in March and to about 410 Dobson at 60°S in October. A small minimum (380 Dobson) is seen over the South Pole during spring and is associated with the presence of a strong vortex (and consequently inhibited meridional transport) around the Antarctic continent from June to October. When the model is run at steady state for 1990 conditions (chlorine level of 3.52 ppbv), similar patterns are produced by the model (see Figure 3*b*) but with substantial depletion over the South Pole in spring. Figure 3*c* shows that the relative difference between the ozone column abundances predicted for 1970 and 1990 are small at low latitudes and midlatitudes. Between 30° and 60°N, even a slight increase is found during all seasons, as a result of changes in the level of CO_2 and CH_4. South of 45°S, substantial depletion is predicted (4% at 44°S up to 40% at 85°S in October). A decrease of less than 2% is calculated at the North Pole in March.

An inspection of the model output (not shown) indicates that, at the beginning of the polar night, the chemistry is significantly perturbed in both hemispheres: NO_2 is converted into N_2O_5 which is further converted into HNO_3. When type II PSCs are present (which is the case mostly in Antarctica), the atmosphere is progressively denitrified. These processes lead to a large decrease of both HNO_3 and NO_2 column abundances in the vortex, with values of 10^{16} cm^{-2} (HNO_3) and 3×10^{15} cm^{-2} (NO_2) outside the vortex and values as low as 6×10^{15} cm^{-2} (HNO_3) and 4×10^{14} cm^{-2} (NO_2) inside the vortex.

In the northern hemisphere, type II PSCs are only present for a brief period in late January and early February, between 24 and 26 km, leading to local decreases in the HNO_3 densities. Otherwise, the heterogeneous conversion of N_2O_5 into HNO_3 takes place on type I PSCs and leads to an increase in the HNO_3 densities around 20 km, together with a decrease in the NO_2

TABLE 2. Assumed History of Trace Gas Concentrations

	1960	1965	1970	1975	1980	1985	1990
CO_2, ppmv	316	321	327	333	339	345	352
N_2O, ppbv	289	292	295	298	302	306	310
CH_4, ppbv	1255	1316	1375	1450	1525	1600	1675
CH_3Cl, pptv	600	600	600	600	600	600	600
CCl_4, pptv	75	80	85	90	95	100	105
CH_3CCl_3, pptv	5	30	55	80	105	130	150
CFC-11, pptv	11	27	60	116	173	220	275
CFC-12, pptv	33	64	121	207	297	375	468
CFC-113, pptv	0.2	0.8	2.3	6.3	15.3	30	51
CFC-114, pptv	0.2	0.6	1.4	2.4	3.8	5	7
CFC-115, pptv	0	0	0.2	0.8	2.1	4	5
CFC-22, pptv	1	4	10	27	54	80	111
Halon-1211, pptv	0	0	0.1	0.2	0.5	1.5	1.8
Halon-1301, pptv	0	0	0.1	0.2	0.6	1.7	3.2
Total Cl_x, ppbv	1.02	1.23	1.55	2.01	2.52	2.98	3.52

density. Total HNO_3 maximum abundances of the order of 1.5×10^{16} cm^{-2} are obtained near the North Pole, while at the same time, the NO_2 abundance reaches values as low as 4×10^{15} cm^{-2}. Observations made during January and February 1989 in the Arctic regions have indicated similar enhanced and reduced abundances of HNO_3 (up to 3×10^{16} cm^{-2}) and NO_2 (3×10^{14} cm^{-2}), respectively [*WMO*, 1990].

When PSCs are present in the lower stratosphere, the chlorine reservoirs HCl and $ClONO_2$ are converted into forms of chlorine that can react with ozone. Over the Antarctic region, in September, the calculated ClO abundance reaches up to 1 ppbv at 23 km and 0.6 ppbv at 18 km (Figure 4*a*); this latter value is consistent with the mixing ratio measured at 18 km in the polar vortex during the Airborne Antarctic Ozone Experiment campaign (maximum mixing ratios between 0.55 and 1.2 ppbv [*Brune and Anderson*, 1989*a*; *Anderson et al.*, 1989]. BrO also increases in the vortex where it reaches 6 pptv near 20 km altitude [*Brune and Anderson*, 1989*b*].

In the Arctic, the coldest temperatures are found only in the 24–26 km altitude range in late January and February and do not reach the threshold under which type II PSCs are formed. Denitrification is therefore limited, and the calculated mixing ratio of ClO reaches only 0.6 ppbv, near 22 km altitude (Figure 4*b*). It disappears through a reaction with NO_2, which is produced by photolysis of nitric acid.

The destruction of ozone over Antarctica by chlorine and bromine begins as soon as sunlight returns to the polar regions. The evolution with time of the ozone column calculated for a level of chlorine equal to 3.5 ppbv is shown in Figure 3*b*. At the South Pole, the ozone column decreases by nearly 40% from 325 Dobson at the beginning of August to 200 Dobson in October. Such reductions have been observed in the mid-1980s [*Hofmann et al.*, 1989; *Komhyr et al.*, 1988; *Gardiner*, 1988] and have even become more dramatic at the end of the decade as the level of Cl_x continued to increase.

The relationship between the presence of chlorine monoxide and the destruction of ozone in the Antarctic region is illustrated by Figures 5*a* and 5*b*. On August 15 (Figure 5*a*), the mixing ratio of ClO at 21 km, which is lower than 5 pptv outside the chemically perturbed region, is already enhanced (40 pptv) in the sunlit air masses included in the polar vortex. At that time, ozone is not yet affected since its loss rate is still too small to destroy significant amounts of this gas in a relatively short period of time. On October 14 (Figure 5*b*), the mixing ratio of chlorine monoxide at 21 km has reached values of the order of 750 pptv south of 70°S and the level of ozone (originally 2.2 parts per million by volume (ppmv)) is now below 0.5 ppmv. The same type of anticorrelation between O_3 and ClO has been observed from the ER-2 aircraft during the 1987 Airborne Antarctic Ozone Experiment [*Anderson et al.*, 1989].

The change in the vertical profile of the ozone density calculated from July 31 to October 29 is shown in Figure 6. The ozone-depleted layer ranges in the vertical from 12 to 26 km and is thus somewhat broader than suggested by the observations (12 to 22 km). However, in agreement with measurements [*Hofmann et al.*, 1988], the ozone density at 21 km (5×10^{12} cm^{-3} on July 31; 0.5×10^{12} cm^{-3} on October 14) is reduced by 90 percent during the ozone hole episode.

In the northern polar region, where elevated concentrations of ClO are predicted during a period of time substantially shorter than in Antarctica, the ozone destruction calculated in the lower stratosphere is limited. Such results are consistent with observations made in the Arctic, where no ozone hole is reported. The model, however, does not explicitly reproduce the dynamical features associated with the evolution of the polar vortex nor the mechanisms by which large volumes of air can be chemically processed by a limited volume of polar stratospheric clouds. Thus, two-dimensional models, even with detailed parameterizations for heterogeneous chemistry in polar regions, are not expected to simulate accurately processes such as the dilution of vertical air toward lower latitudes or potential exchange of air through the boundary of the vortex.

Finally, the evolution since the early 1960s of the springtime ozone column abundance is simulated by the model, based on the observed trend of CO_2, CH_4, N_2O, and the CFCs. During this period, the total chlorine amount has been increased by a factor of about 3, and CO_2, CH_4 and N_2O have increased at yearly rates of approximately 0.4%, 1%, and 0.25% respectively [*WMO*, 1990].

The total ozone abundance at 85°S, calculated during mid-October from 1960 to 1990, is compared in Figure 7 with the October mean ozone column measured at the South Pole [*WMO*, 1990] in Antarctica. The computed total ozone amount has decreased by a value similar to the observed reduction (200 Dobson) but never reaches the very low ozone columns observed in October 1987, 1989, and 1990 (approximately 140 Dobson). Furthermore two-dimensional models do not reproduce interannual variability associated with fluctuating meteorological conditions.

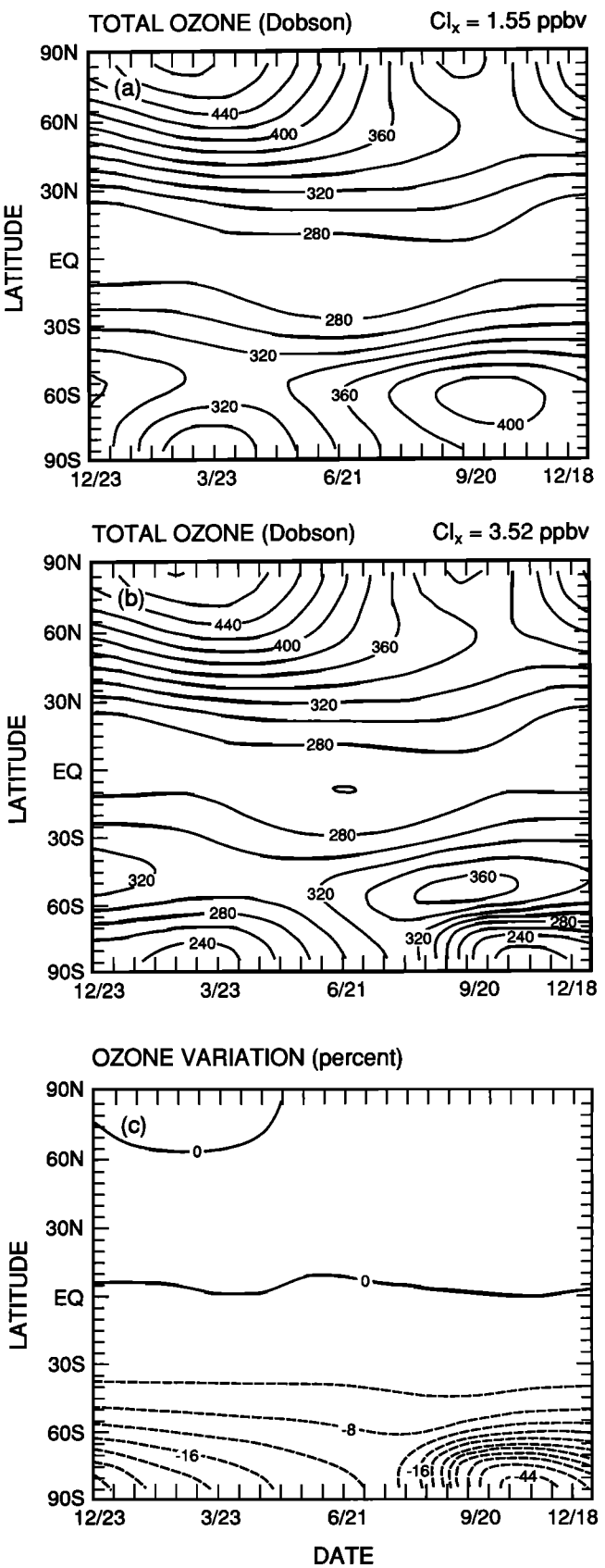

Fig. 3. Calculated ozone column abundance (Dobson) as a function of latitude and time of the year: (*a*) level of chlorine is 1.55 ppbv, (*b*) level of chlorine is 3.52 ppbv, and (*c*) relative difference expressed in percent between Figures 3*b* and 3*a*. The chemistry associated with the presence of polar stratospheric clouds is taken into account. The impact of sulfate aerosols is ignored.

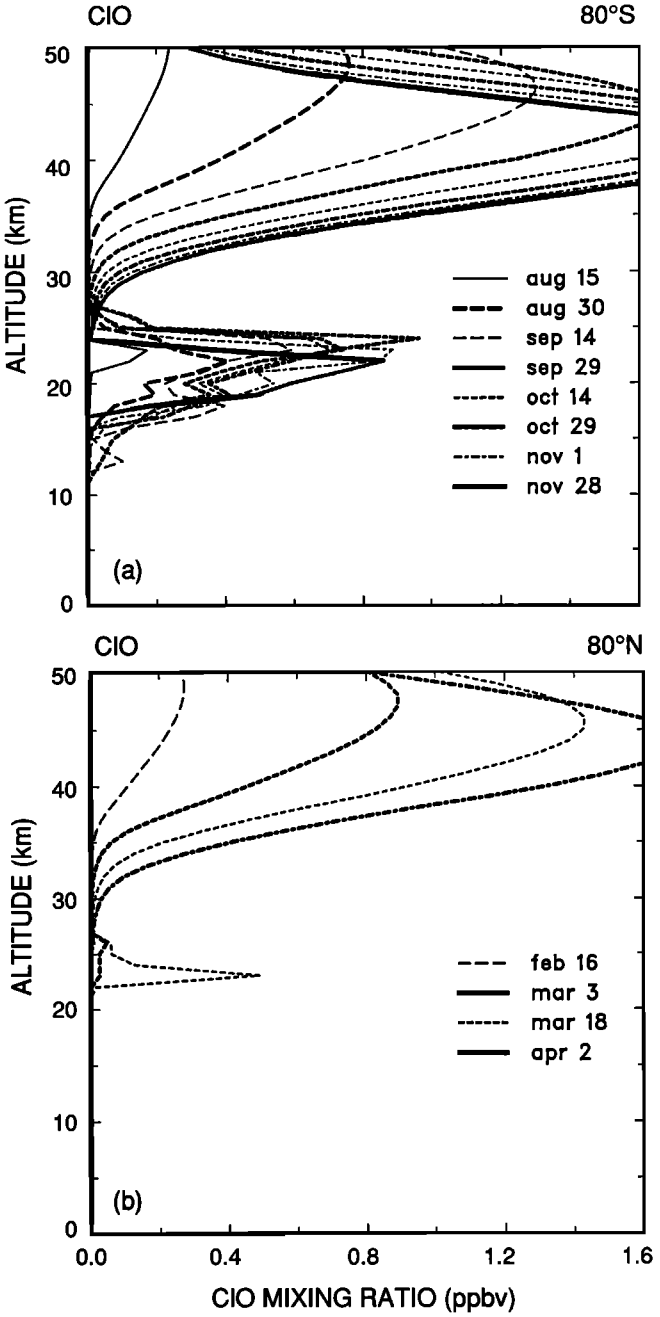

Fig. 4. Calculated mixing ratio of ClO (in ppbv) for different times of the year: (*a*) profiles at 80°S, and (*b*) profiles at 80°N.

In conclusion, the formulation of polar chemistry in the model produces the main features of the past year's observations concerning the ozone distributions with some differences probably associated with the two-dimensional character of the model formulation. Ozone is the only species for which routine measurements are available in the polar regions, so no detailed comparison can be made of the evolution over the past 20 years of other minor stratospheric species.

5. The Effects of Stratospheric Sulfate Aerosols

Heterogeneous processes in the lower stratosphere modify the relative abundance of NO_y and Cl_x species and consequently affect the concentration of ozone. Because nitrogen oxides are

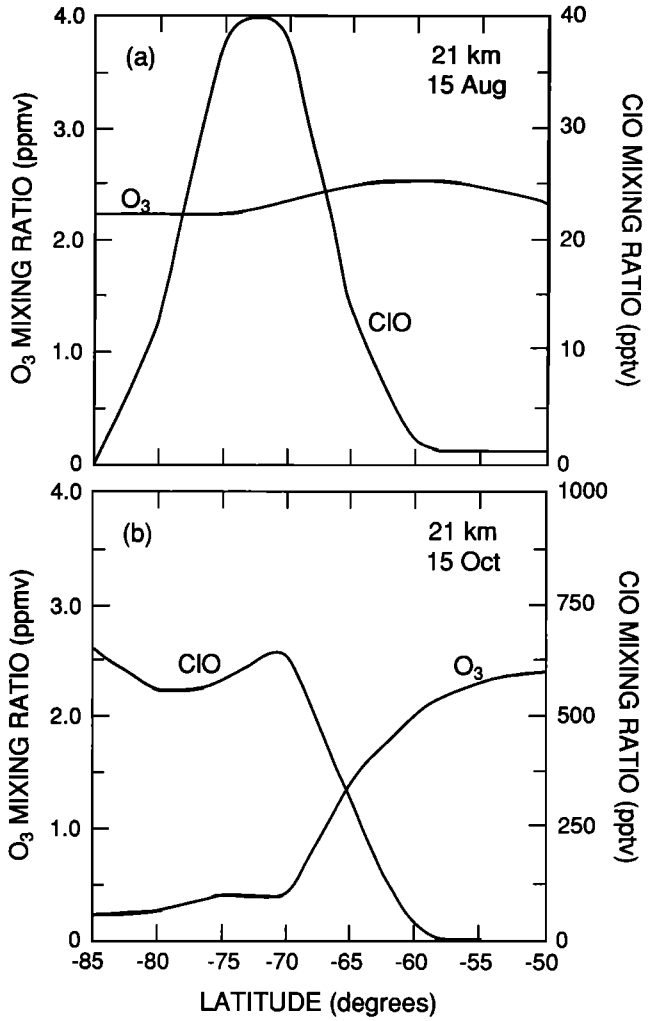

Fig. 5. Mixing ratio of ClO (pptv) and O_3 (ppmv) as a function of latitude in the vicinity of the Antarctic vortex: (*a*) latitudinal profiles on August 15, and (*b*) latitudinal profiles for October 14.

converted into nitric acid, and chlorine nitrate into more reactive forms of chlorine, these processes tend to shift the atmosphere from a situation in which ozone is primarily controlled by the oxides of nitrogen to a situation in which the ozone loss becomes largely affected by the chlorine compounds.

Reaction (1) influences the chlorine partitioning directly, while reaction (2), which affects primarily the budget of nitrogen oxides, modifies the chlorine partitioning indirectly. As N_2O_5 is converted into HNO_3, the abundances of NO_2 and NO are reduced, and hence the recombination of ClO with NO_2 to form $ClONO_2$ becomes less efficient. Thus, the concentration of ClO should be enhanced as a result of reaction (2). The rate of reaction

$$ClO + NO \rightarrow Cl + NO_2$$

is also reduced, and hence the destruction rate of ozone by chlorine is enhanced. Finally, the heterogeneous conversion of nitrogen oxides into nitric acid produces an increase in the concentration of the OH radical, since the homogeneous formation of HNO_3,

$$NO_2 + OH + M \rightarrow HNO_3 + M$$

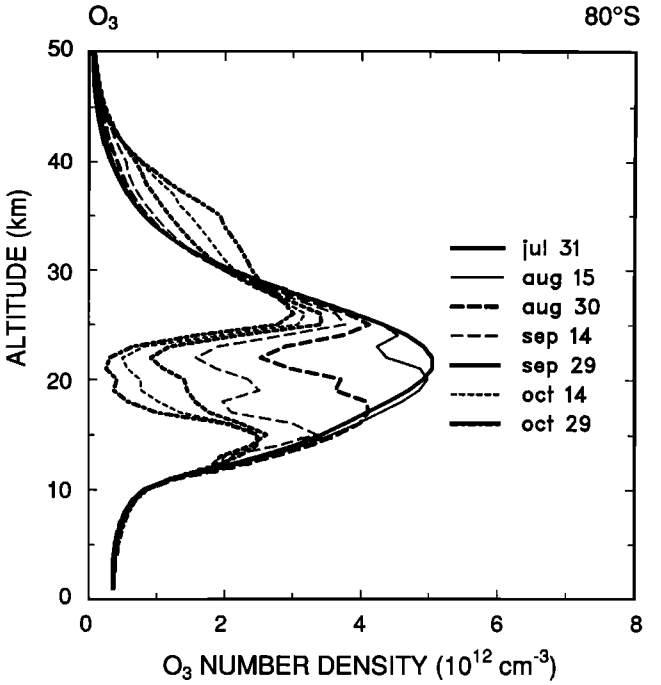

Fig. 6. Calculated density of ozone (cm^{-3}) at 80°S between July 31 and October 29.

which destroys OH radicals indirectly competes with reaction (2) which also converts NO_x into HNO_3 but does not destroy OH. Hence, the conversion rate of HCl into reactive chlorine,

$$HCl + OH \rightarrow Cl + H_2O$$

is enhanced.

5.1. *Background Conditions*

Figures 8*a* and 8*b* show the conversion rate of $ClONO_2$ and N_2O_5 to HNO_3, respectively, as a function of altitude and latitude, assuming a background aerosol load. In the case of N_2O_5 (Figure 8*b*), the heterogeneous conversion occurs over a couple of days in the region where the aerosol surface area

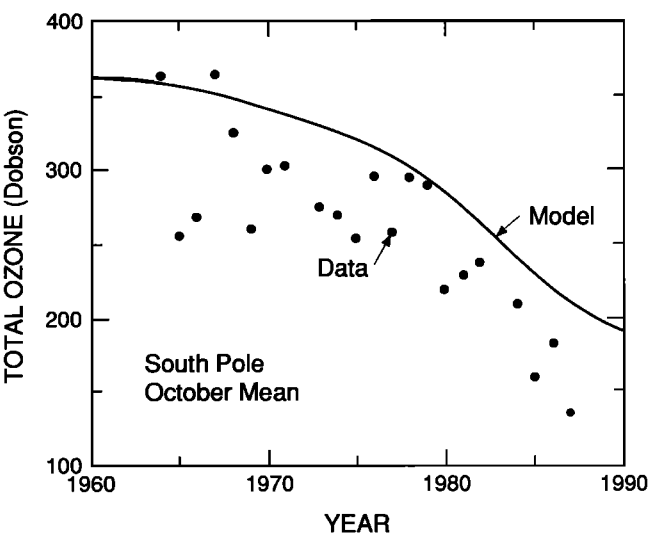

Fig. 7. Variation between 1960 and 1985 of the October mean total ozone abundance at 85°S.

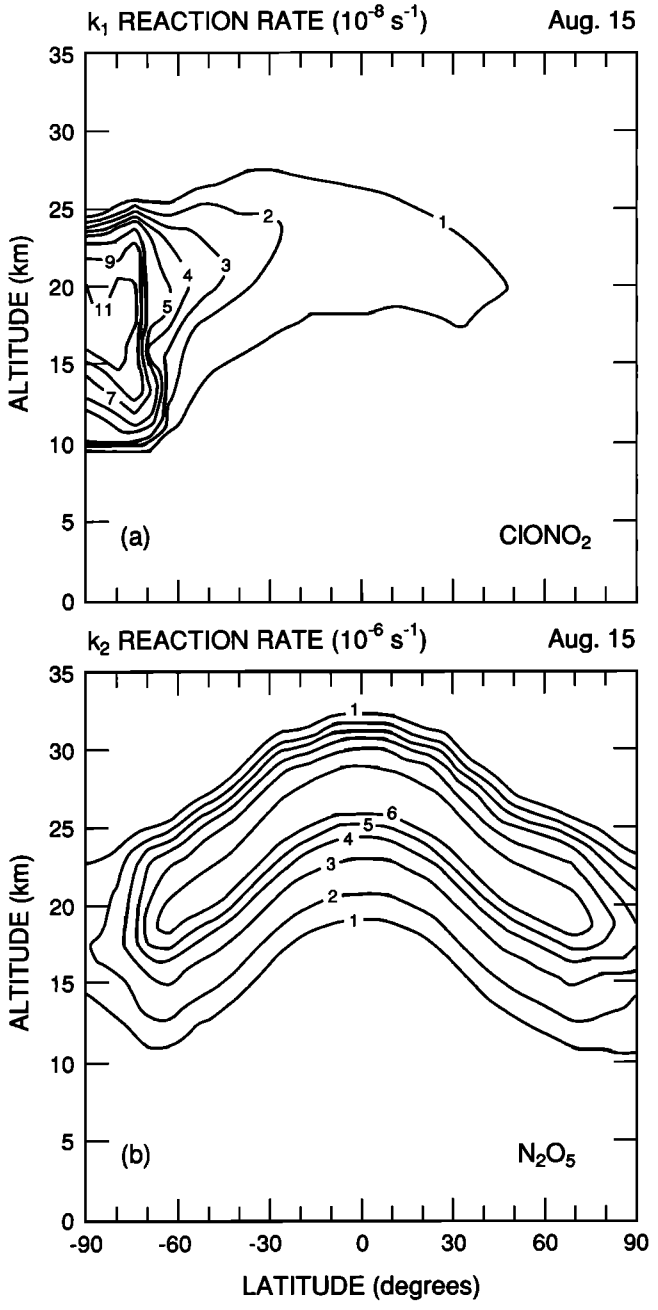

Fig. 8. Conversion rate (s^{-1}) of (*a*) $ClONO_2$ and (*b*) N_2O_5 on background sulfate aerosols in the lower stratosphere. Values are shown as a function of latitude and altitude.

density (A) reaches its maximum of 0.7 μm^2 cm^{-3}. The rate of conversion is essentially proportional to A. In the case of $ClONO_2$, the conversion rate is also dependent on the composition of the aerosol and hence on the temperature and water mixing ratio of the atmosphere. Thus, in the coldest air masses where the reaction probability of reaction (1) is largest, the conversion of $ClONO_2$ is most efficient. As shown in Figure 8*a*, the heterogeneous conversion is fastest in the winter polar stratosphere where it occurs in 3 to 4 months and can therefore play a significant role. It should be noted that reaction (1) also contributes to the transfer of nitrogen oxides into nitric acid. As HOCl released by this reaction is photolyzed to produce Cl and OH radicals, it is expected that the effect of this reaction on ozone will be most pronounced in the subpolar regions during winter and in the polar regions after the return of sunlight in spring.

In summary, based on measured reaction probabilities, reaction (2) is the most efficient of the two heterogeneous mechanisms associated with sulfate aerosols both globally and at low latitudes and midlatitudes, but reaction (1) eventually plays a substantial role at high latitudes during winter when the temperature of the stratosphere is low.

The relative changes in the concentrations of key stratospheric species for a background aerosol load are shown in Figures 9*a*–9*d* for the month of April. In the case of nitric acid (Figure 9*a*), an increase of up to 90 percent (almost a doubling) is predicted by the model at high latitudes near 20 km altitude. In the tropics, the changes are smaller but still significant, especially at 25 km altitude. The vertical profiles of the HNO_3 mixing ratio calculated at 70°N on February 1, when the effects of sulfate aerosols are either taken into account or ignored, are shown in Figure 10*a*. The agreement with observations is significantly improved when the effects of aerosols are taken into account. The mixing ratio calculated for February at 70°N and 24 km is enhanced from 5 ppbv to 8.5 ppbv with the introduction in the model of heterogeneous chemistry (aerosols), while the mixing ratio observed at 68°N by the Limb Infrared Monitor of the Stratosphere (LIMS) on board the Nimbus 7 satellite (J. Gille, personal communication, 1992) is in February equal to 9.5 ppbv at the same altitude. Note that the height of the HNO_3 peak also agrees better with observation when the heterogeneous conversion of N_2O_5 is taken into account. In the case of NO_2 (Figure 9*b*), a large reduction is found, particularly at high latitudes. Nitrogen dioxide (as well as nitric oxide, not shown) is virtually removed in the lower stratosphere, as shown for 70°N in Figure 10*b*. A comparison with the LIMS data shows that the calculated 24-hour average of the NO_2 mixing ratio is lower than that observed during daytime and that the NO_2 concentration is even further away from the observed one when heterogeneous processes are added to the chemical scheme in the model.

The same conclusions are reached from an inspection of Figure 11. The variation with latitude of HNO_3 observed by LIMS at 50 mbar is best reproduced by the values calculated at 20 km when the heterogeneous conversion of N_2O_5 is taken into account (Figure 11*a*). On the contrary, the LIMS measurements are closer to the gas phase model of NO_2 than to the model accounting for aerosol effects (Figure 11*b*). If nighttime NO_2 measured by LIMS is compared to the ($NO+NO_2$) concentrations provided by the model, the calculated mixing ratios agree best (in absolute values) with the heterogeneous chemistry case, but in terms of latitudinal variation, the mixing ratios agree with the homogeneous chemistry case (Figure 11*c*). As noted by *Considine et al.* [1992], the $(NO+NO_2)/HNO_3$ concentration ratio, which is largely independent of the level of odd nitrogen compounds in the atmosphere, reflects the conversion rate of nitrogen oxides into nitric acid. The best agreement between the theoretical curve and the curve deduced from LIMS data is achieved when heterogeneous reactions are included in the model (Figure 11*d*). When, however, the NO_2/HNO_3 concentrations are compared (not shown), the values deduced from observational data are closest to the values calculated in the case when only gas phase processes are taken into account. This last result is consistent with the calculations of *Considine et al.* [1992] reported for the 29 mbar level. Note that, at the altitude of 20 km, the

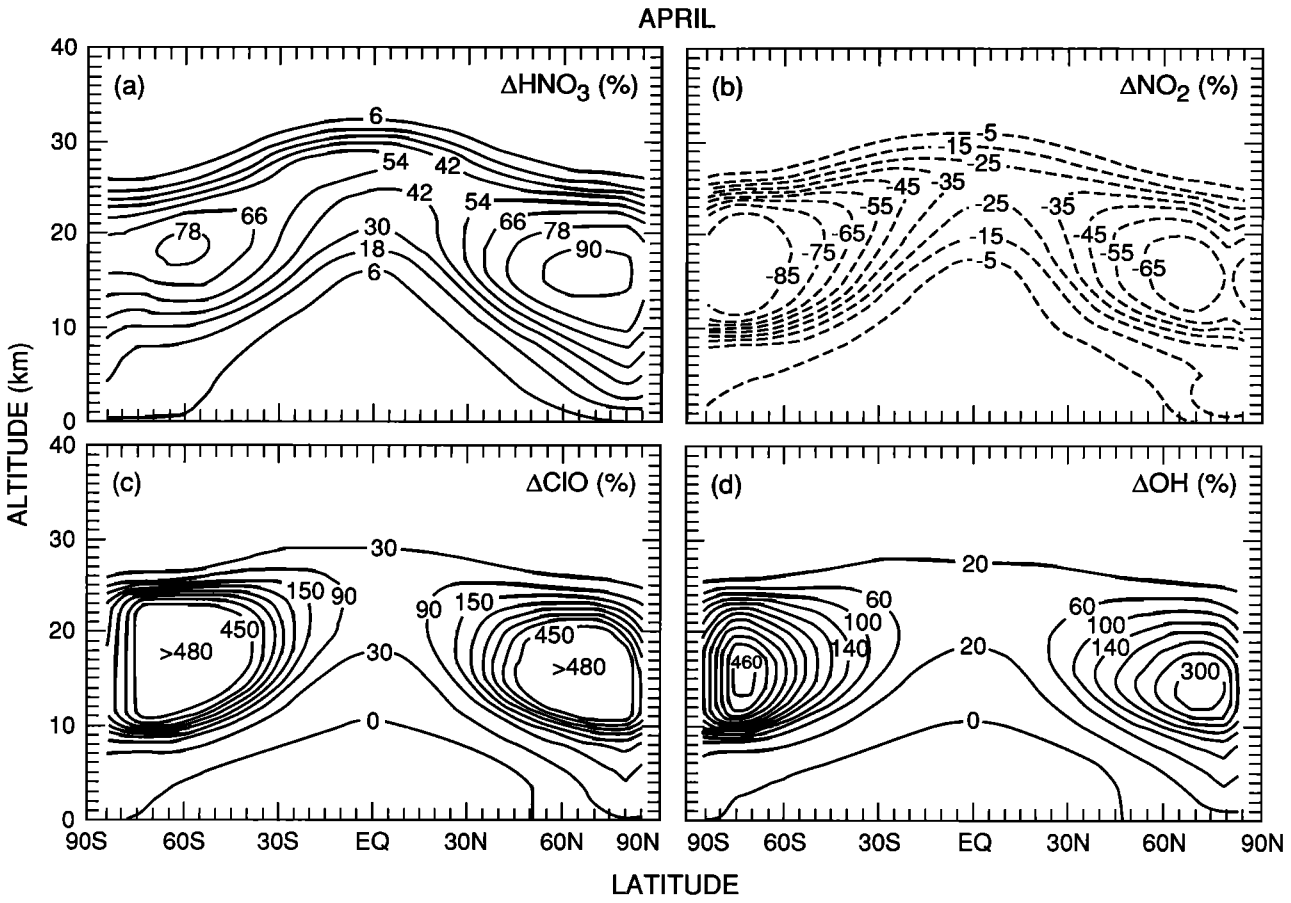

Fig. 9. Relative change (percent) in the concentration of (*a*) HNO_3, (*b*) NO_2, (*c*) ClO, and (*d*) OH shown as a function of latitude and altitude for the month of April, associated with heterogeneous reactions on sulfate aerosols (background aerosol load).

difference between the observed day and night concentrations of NO_2 (which essentially represents the concentration of daytime NO) is significantly smaller than in the model. This discrepancy, which might not be related to heterogeneous conversion processes, limits our ability to validate the scheme from which heterogeneous reactions rates are estimated. Uncertainties in the calculation of these rates include a possible saturation effect by which the aerosol becomes inefficient in converting N_2O_5 and $ClONO_2$ after it has already undergone several of these reactions. An overestimation of the reaction probability for reaction (2), or of the aerosol surface area for background conditions, could also explain the discrepancy between observed and calculated NO_2 concentrations in the lower stratosphere. Laboratory work is needed to quantify the reaction probabilities under all possible atmospheric conditions, especially for a H_2SO_4/H_2O weight ratio larger than 80 percent. Other possible problems need to be elucidated, such as the products of reaction (2) which have not been measured in the laboratory and could be more reactive compounds than HNO_3. Also, the fact that models derive concentrations of total NO_y that are lower than what is measured may indicate that there is an additional, unidentified source of NO_y in the lower stratosphere. Comparisons between models and observations should involve data gathered over several years (not yet available on the global scale) since the quasi-biennial oscillation of the atmosphere affects the observed concentration of nitrogen compounds, particularly in the tropics near 20 km altitude.

The percentage change in ClO, shown in Figure 9*c*, suggests that a large perturbation also takes place in the chlorine family. The level of ClO is extremely low (less than 1 pptv at 20 km) when calculated for homogeneous chemistry but reaches values as high as 100 pptv when heterogeneous conversion is included in the model. Such values should be detectable and large enough to substantially affect the ozone budget in the lower stratosphere. The change in the concentration of the OH radical, shown in Figure 9*d*, is a direct consequence of the shift from a "NO_x-controlled atmosphere" to a "ClO_x-controlled atmosphere." As a result, a relatively large number of stratospheric constituents are indirectly affected by the presence of aerosols.

Finally, the change in the ozone concentration resulting from the perturbation in the NO_x, ClO_x and HO_x chemistry is shown in Figures 12*a* and 12*b*. In the region above 15 km, the introduction of heterogeneous chemistry leads to an increase in the ozone concentration, associated with the reduction in the ozone loss by NO_x. Near the tropopause, where the ozone destruction is also largely controlled by the HO_x chemistry (and now also by ClO_x), the concentration of ozone is reduced. The "crossover point" between regions of ozone increase and decrease varies with season and with the level of total chlorine assumed in the model. In late winter, when reaction (1) is efficient and the direct destruction of ozone by chlorine is largest, the transition point is as high as 25 km altitude.

The vertical profiles of ozone are only slightly changed by the effects of heterogeneous reactions on sulfate aerosols,

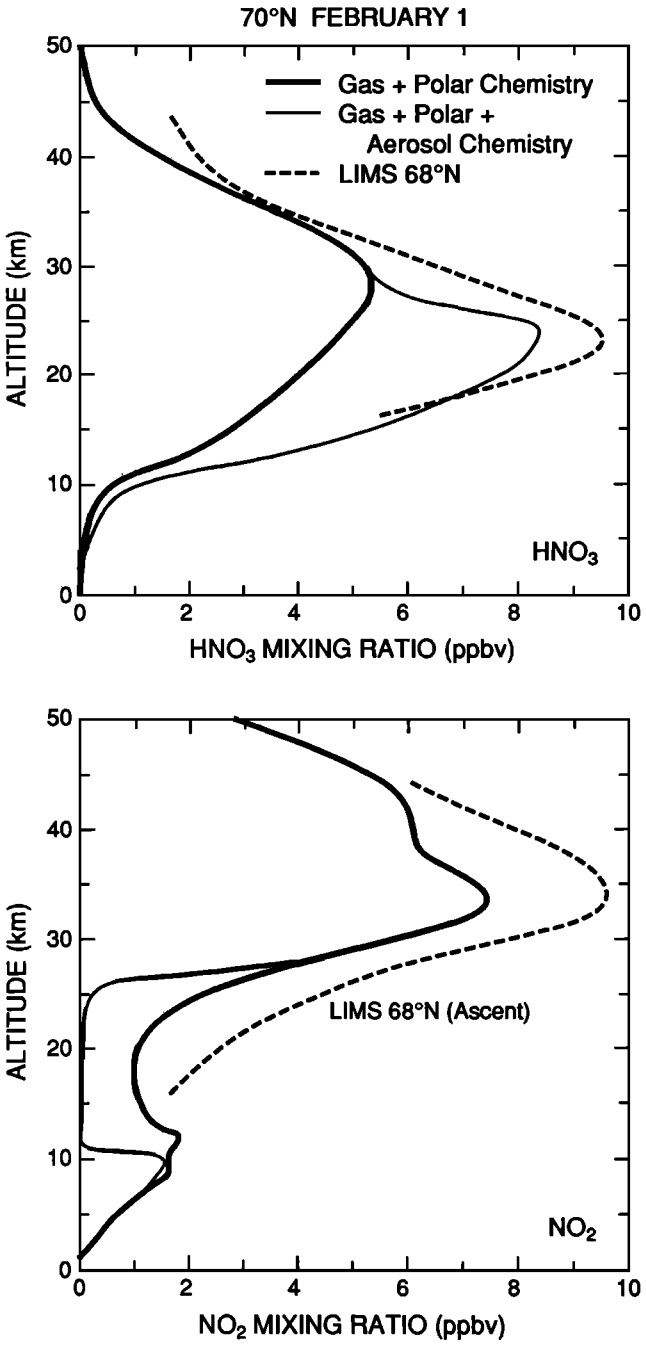

Fig. 10. Vertical distribution at 70°N in February of HNO_3 (ppbv) and NO_2 (ppbv) when heterogeneous chemistry on sulfate aerosols is ignored and taken into account. Data from LIMS at 68°N (monthly mean values) are also shown.

under background conditions, and for a Cl_x level equal to 3.5 ppbv (see Figure 12*b*). The corresponding perturbation on the ozone column abundance is of the order of a few percent, particularly at low-latitudes and mid-latitudes (see Figures 13*a* and 13*b*). If the contribution of the $ClONO_2$ conversion is ignored (Figure 13*a*), the ozone column increases by up to 5 percent, except in the polar regions during winter, where decreases of less than 3.5 percent are derived from the model (Figure 13*b*). When the effects of both heterogeneous conversions are included in the model, a slight increase in the ozone column is still found, but the winter high-latitude ozone reduction is now characterized by larger values (up to 15 percent in the southern hemisphere where the coldest air masses are located). It might be worth noting at this point that the effects of sulfate aerosols and polar stratospheric clouds have been treated independently in the model, ignoring the potential condensation of water and nitric acid on the aerosol nuclei. The "additional" reduction in total ozone calculated in the polar regions when sulfate aerosols are included results from the destruction of ozone molecules between primarily 8 and 15 km altitude, a layer in which only a few PSCs are produced in our model simulations.

5.2. *Postvolcanic Conditions*

In June 1991, after 635 years of inactivity, the Philippine volcano Mount Pinatubo (15.4°N) erupted, and approximately 15–20 Mt of SO_2 [*Bernard*, 1991] were injected into the atmosphere, causing the formation of a large aerosol cloud which immediately reached an altitude of 25–30 km. The surface area available for heterogeneous processes to occur in the stratosphere has therefore substantially increased, first in the tropics where the cloud remained confined for several months after the eruption and, later, in the entire northern and southern hemispheres after dispersion of the cloud by the general circulation of the atmosphere. Following large volcanic eruptions, the concentration of nitrogen oxides in the lower stratosphere should decrease while that of nitric acid and active chlorine (Cl, ClO) should increase. Observations made after the eruption of El Chichón in 1982 suggest that significant amounts of nitrogen oxides have been converted into nitric acid [*Roscoe et al.*, 1986] and that ozone has been depleted substantially at mid-latitudes, mostly in the 18–21 km altitude layer (see *Hofmann and Solomon* [1989] for a review of ozone observations). Because the amount of sulfur injected by El Chichón has been estimated to be 2 to 3 times lower than that emitted by Pinatubo, and because the level of chlorine in the early 1980s was approximately 30 percent lower than in 1991, the perturbations following the recent eruption of the Philippine volcano are expected to be more intense and to last longer.

Detailed microphysical and transport models are required to estimate as a function of time and space the surface area density associated with the volcanic cloud. S. Bekki and J. Pyle (1992), using the aerosol model of *Turco et al.* [1979] coupled to their two-dimensional chemical/transport model, have estimated that the maximum surface area density should reach values larger than 10 $\mu m^2\ cm^{-3}$ in the entire northern hemisphere several months after the eruption. The dilution of the cloud appears, however, to be more complex than simulated by two-dimensional models [*Boville et al.*, 1991] so that, at this stage, only simple assumptions can be made on the fate of the volcanic material. It seems, for example, that contrary to what happened after the eruption of El Chichón, a large fraction of the aerosol material has been transported into the southern hemisphere. Since the distribution as a function of time of the surface area density is poorly known, we have constructed distributions of this parameter based on available observations, assuming that the volcanic cloud is globally dispersed. For example, in the case of El Chichón (Figure 14), the observations used include the measurements of surface area densities made above Laramie (41°N) in January 1983 (see Figure 2) and presented by *Hofmann and Solomon* [1989] and the measurements of the aerosol column density performed by *McCormick et al.* [1984] from 57°S to 72°N in May 1983. The distribution shown in Figure 14 is not intended to reproduce the

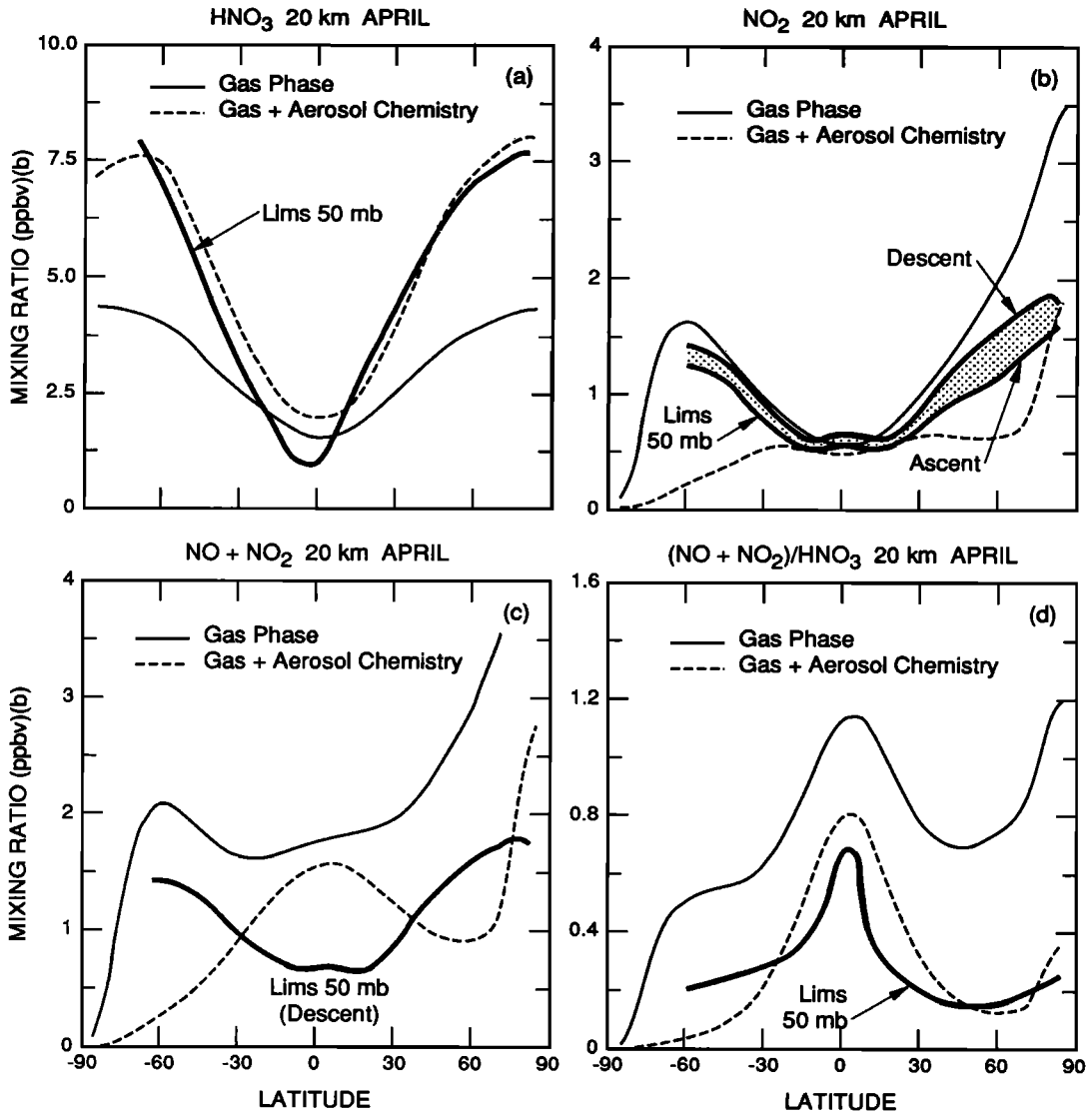

Fig. 11. Volume mixing ratio of (*a*) HNO_3, (*b*) NO_2, (*c*) $NO+NO_2$, and (*d*) $(NO+NO_2)/HNO_3$ concentration ratio calculated as a function of latitude at 20 km altitude (April) for different conditions. Values are compared with values deduced from LIMS observations. Note that in Figure 11*b* the shaded area includes daytime and nighttime NO_2 data, while in Figure 11*c*, only nighttime NO_2 LIMS data are shown. The ratio shown in Figure 11*d* for LIMS data is based on nighttime values of NO_2 concentrations.

exact zonally averaged distribution of the aerosol surface area after the dispersion of the volcanic material but to provide working values to qualitatively estimate the potential impact on the global scale of eruptions similar to that of El Chichón. The values adopted are largest in the northern hemisphere where most of the volcanic material injected by the Mexican volcano was transported; they reach 10 μm^2 cm^{-3} approximately 6 km above the tropopause. Note that in the present discussion, we assume that the distribution of surface area density remains unchanged during the entire year over which the model is integrated, while in the atmosphere, the *e*-folding time for aerosol removal is probably of the order of 1–2 years [*McCormick and Veiga*, 1992].

Figure 15 shows the relative change in the ozone column abundance resulting from the volcanic perturbation, as applied to the model. In this calculation, the level of chlorine is equal to 2.6 ppbv and is thus representative of the early 1980s. As the changes derived for the southern hemisphere are insignificant, only the values calculated north of the equator are shown. The reduction in the ozone column appears to be less than 1 percent in the tropics but increases rapidly with latitude, especially during the winter and spring season. At mid-latitudes (45°N) the calculated depletion is equal to 2.5 percent in winter and approximately 1.5 percent in summer and fall. The largest depletion is 10 percent near 75°N in February. When the calculation is redone with a level of chlorine of 3.5 ppbv, representative of the early 1990s, but with the same aerosol surface area density, the pattern of the ozone changes looks similar, with a depletion that now reaches 13 percent at 75°N in February. Finally, if the aerosol surface area is doubled and the level of chlorine is that of 1990, the largest reduction in the ozone column abundance reaches 23 percent. In this case, the ozone depletion at 30°N is approximately 2 percent. Thus, although the response in the ozone column is not perfectly linear with surface area or chlorine level, it is very sensitive to these factors, so that the potential effects of the

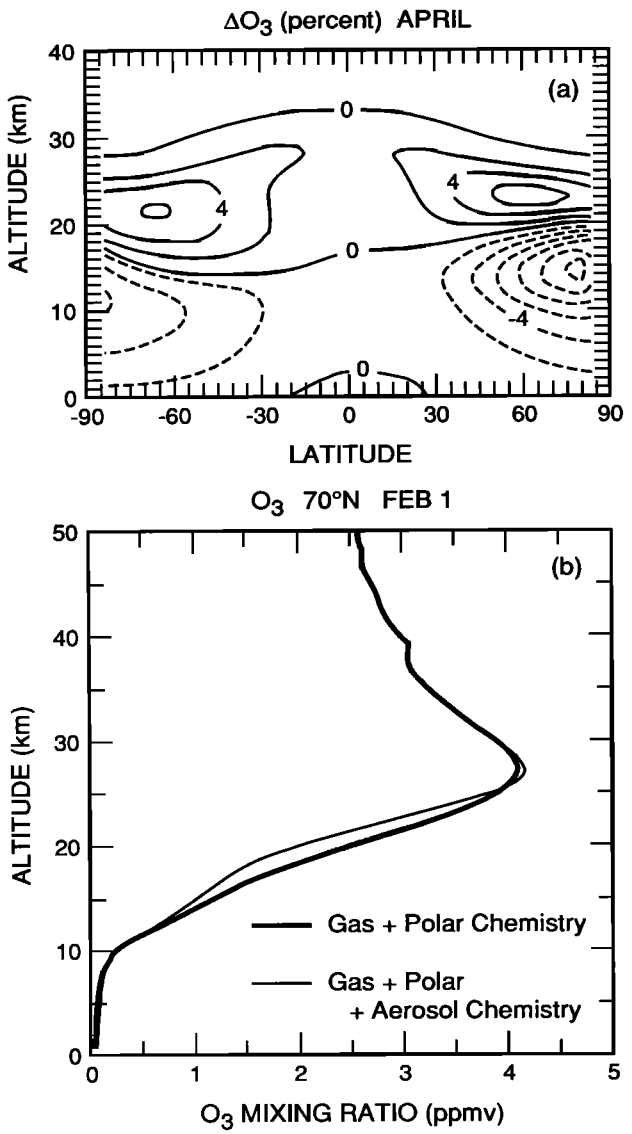

Fig. 12. Same as Figure 9*a* and Figure 10*b* but for ozone.

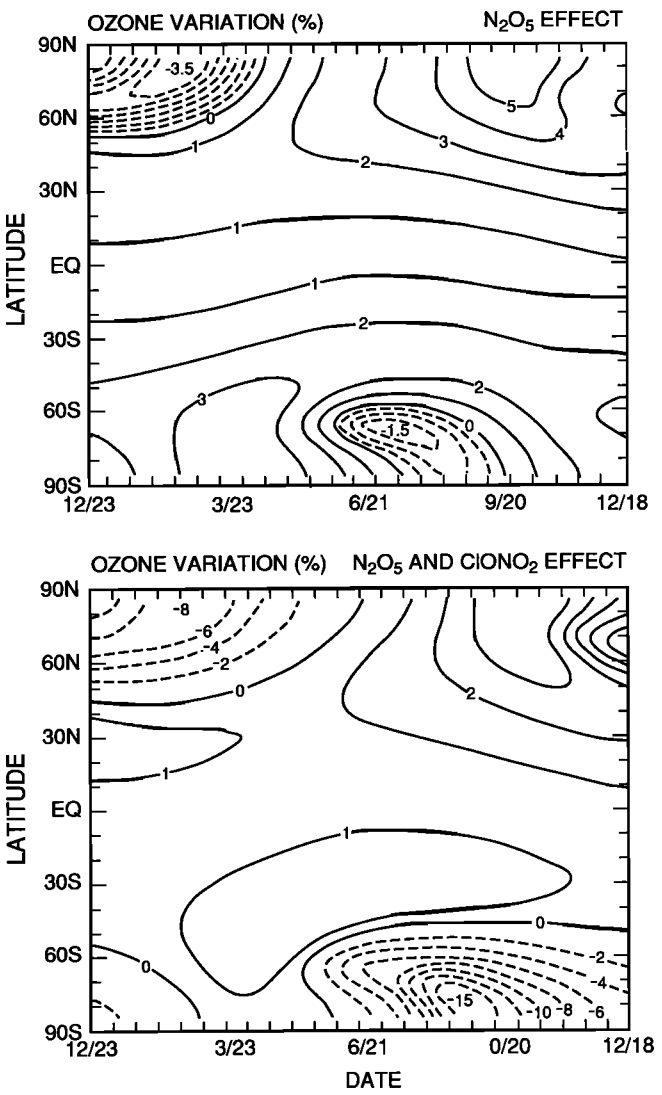

Fig. 13. Relative change (percent) in the ozone column abundance when heterogeneous chemistry on sulfate aerosols is taken into account. (*a*) Effect on the N_2O_5 conversion only. (*b*) Effect on N_2O_5 and $ClONO_2$ conversions.

Pinatubo eruption should be substantially larger than that of El Chichón and should be easily detectable.

In order to simulate the chemical effect of an eruption as powerful as that of Mount Pinatubo (again, after global dispersion of initial clouds), a second distribution of the surface area density has been constructed (Figure 16). This distribution accounts for the fact that the volcanic material has been dispersed in both hemispheres more evenly than in the case of the El Chichón cloud and that the amount of sulfur injected is at least twice as large as during the El Chichón explosion. In this case, we assume as working values that surface area densities reach 16 μm^2 cm^{-3} in the tropics and that they decrease after January 1992 with an *e*-folding time of 15 months.

The relative variation in the ozone column abundance resulting from this volcanic perturbation is shown in Figure 17*a*. Again, the ozone depletion on the global scale is relatively small in the tropics, but it increases towards the poles, with the most pronounced gradients occurring at the end of the winter. With the assumptions made for the dispersed cloud produced by Pinatubo, the calculated decrease in the ozone column abundance reaches 30 percent near the polar vortices (February in the northern hemisphere and August in the southern hemisphere). In June, 1 year after the eruption, the ozone depletion at mid-latitudes in the northern hemisphere is still of the order of 10 percent. The change in the ozone concentration, shown for early March as a function of latitude and height in Figure 17*b*, suggests that the effect of Pinatubo should be mostly visible at high latitudes below 25 km where the decrease in the ozone concentration could reach locally almost 50 percent. Such quantitative values depend critically on the assumption made for the dispersion of the volcanic aerosol. Observational data are needed before a more detailed analysis can be performed.

6. Past Evolution of Stratospheric Ozone

Analyses of ozone observations made by ground-based Dobson instruments and satellite detectors have shown that the total ozone column abundance has substantially decreased between 1980 and 1990 (see for example, *WMO* [1992] for a

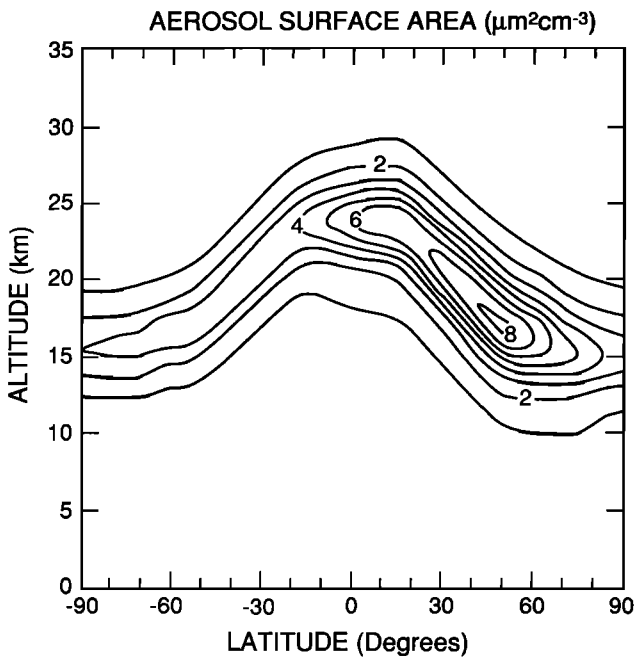

Fig. 14. Surface area density (μm^2 cm^{-3}) adopted as a working value to represent the aerosol load after global dispersion of the El Chichón volcanic cloud.

discussion and *Stolarski et al.* [1991]). In particular, the analysis of the total ozone mapping spectrometer (TOMS) data [*Stolarski et al.*, 1991] suggests that between 65°S and 65°N, the ozone abundance has decreased on the average by 3 percent from November 1978 to May 1990. The ozone reduction is small in the tropics but reaches 30% over the Antarctic continent and 6 percent at 60°S. In the northern hemisphere, the ozone reduction in the 1980s has been of the order of 4–5 percent in the 40° to 60°N latitude belt with values twice as large (8 percent) for the winter season.

The two-dimensional model has been used to simulate potential changes in the chemical composition of the stratosphere between 1980 and 1990. To simplify the calculation, rather than specifying time-evolving emissions of chemical compounds in the atmosphere, steady state simulations have been performed with prescribed surface concentrations of CO_2, N_2O, CH_4, and halocarbons in 1980 and 1990, respectively (see values in Table 2). The calculations (see Figure 18*a*) suggest that, when only gas phase chemistry is taken into account, the change in the column is slightly positive at most latitudes and during most seasons. This results from the increase in tropospheric ozone associated with the prescribed enhancement in the methane concentration and to the reduced ozone destruction rate associated with the moderate stratospheric cooling caused by the increasing CO_2 mixing ratio. The reduction in the ozone column derived at high latitudes in winter is explained by the downward transport of air masses from the upper stratosphere where enhanced chlorine levels tend to reduce the ozone concentration. The results obtained from this model run are in conflict with the trends derived from data analysis [*Stolarski et al.*, 1991].

When the effects of polar chemistry are taken into account, the changes in the ozone column are very different (see Figure 18*b*). In this case, a trend of 30 percent per decade is derived near the South Pole in spring and a decrease of 6 percent per decade is found at 60°S. Thus the model simulation reproduces with some success the trends derived by TOMS south of the equator. The values calculated outside the polar region are highly influenced by the strength of horizontal mixing in the model. This is a major source of error in the simulations since two-dimensional models are not expected to properly reproduce the dilution of ozone-depleted air from the pole to the mid-latitudes.

At the North Pole, where the temperature derived by the model is not sufficiently low to produce type II PSCs, a very limited reduction in the ozone column takes place. As a consequence, the northern hemisphere is not significantly perturbed by polar processes. When, however, the effects of background aerosols are taken into account, a substantial reduction of ozone takes place at midlatitudes and high latitudes in the northern hemisphere (Figure 18*c*). Values of the order of 4–10 percent per decade are predicted in the winter season, while in summer the calculated depletion is less than 4 percent per decade. This result tends to suggest that, even when the level of aerosols corresponds to background conditions, heterogeneous processes on the surface of sulfate particles could significantly contribute to the observed ozone trend. One should emphasize, however, that occasionally in the

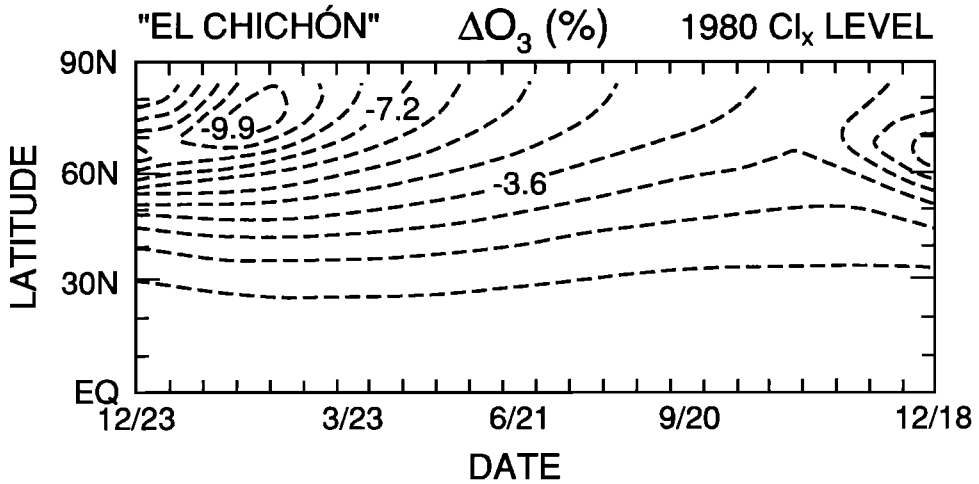

Fig. 15. Relative change (percent) in the ozone column abundance of the northern hemisphere in response to volcanic eruption using the aerosol surface area density shown in Figure 14 with chlorine load representative of the early 1980s. The reference case includes aerosols at background level.

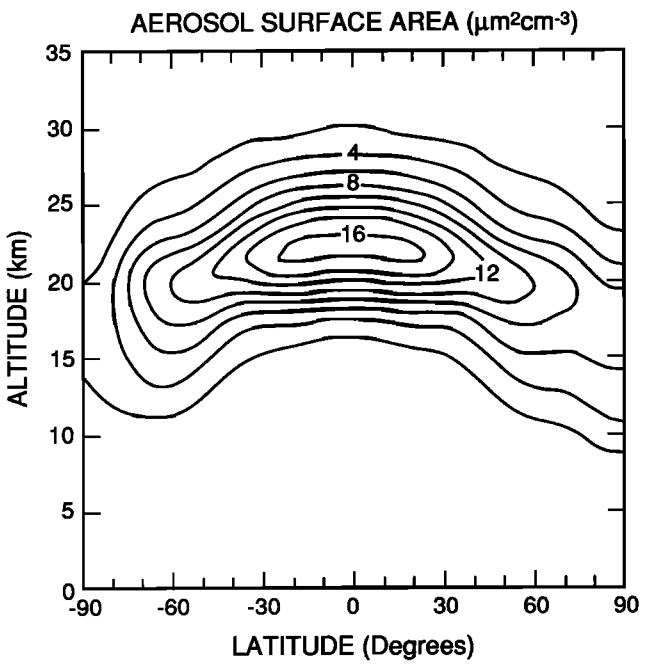

Fig. 16. Same as Figure 14 but for Mount Pinatubo volcanic cloud in January 1992.

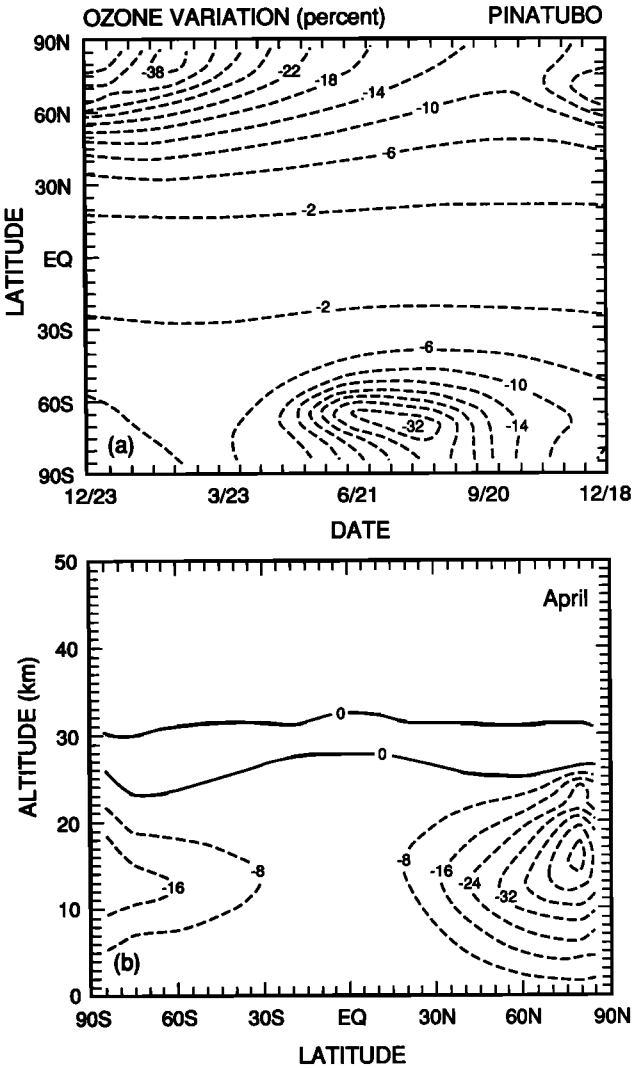

Fig. 17. (*a*) Relative change (percent) in the ozone column abundance calculated in response to the eruption of Mount Pinatubo. Values are shown as a function of latitude and season. Surface area density shown in Figure 16 decreases uniformly after January with an *e*-folding time of 15 months. (*b*) Relative change (percent) in the ozone density as a function of latitude and altitude in March 1992. Reference case includes background aerosols.

Arctic region, polar stratospheric clouds form in localized air masses and that these clouds process enough air to perturb a large fraction of the northern hemisphere. Thus, in spite of the fact that the model does not suggest a strong influence of polar heterogeneous processes on ozone in the northern hemisphere, there is observational evidence that the level of active chlorine is substantially increased in the Arctic region in winter, so that the dilution of perturbed air could lead to large ozone depletion at mid-latitudes in the northern hemisphere. As shown by Table 3, even with the effects of sulfate aerosols taken into account, the model does not properly reproduce the ozone trend seen by TOMS at mid-latitudes in winter, in spite of the fairly good agreement between model and data at other latitudes (including the southern hemisphere) and seasons. Three-dimensional model simulations at high spatial resolution with coupled dynamics, chemistry, and microphysics are needed to fully investigate this question.

7. Conclusions

Parameterizations of the heterogeneous processes occurring either on PSC particles in the polar regions or on sulfate aerosol particles at all latitudes play a major role in the chemistry of stratospheric ozone. The simple but realistic parameterizations of the PSC formation used in our two-dimensional model allow us to reproduce the main features associated with the formation of the ozone hole over Antarctica. No ozone hole is predicted by the model in the early 1960s, but, starting in late 1970s, the springtime ozone decrease is reproduced, at least in qualitative terms. In the polar region of the northern hemisphere, the chlorine is also significantly perturbed, but no "ozone hole" is produced in the model.

The heterogeneous processes on sulfate aerosol particles are also playing an important role. Several uncertainties still exist in the parameterizations of these processes. For example, no experimental data is presently available on the climatology of the aerosol size distribution at all latitudes, so that idealized distributions of the aerosol surface area have to be used in model simulations. The use of experimental distributions, much less uniform in time and space, would provide different results. This is particularly true in the volcanic case, since, after large eruptions, the dispersion of the volcanic cloud by the circulation of the atmosphere is a highly complex problem. Furthermore, the impact of heterogeneous processes on the submicron particles in the aerosol layer is very sensitive to the values of the reactions probabilities including the rate of the $ClONO_2$-sulfate reaction [*Brasseur et al.*, 1990*b*; *Prather*, 1992], and though very recent data are available, major uncertainties as well as the possibility of missing processes remain a matter of concern.

Despite these limitations and the simplifications made in the computations, important characteristics of the effect of heterogeneous processes on background aerosols have been pointed out. The effects of such processes are larger at high latitudes and become more noticeable as the stratospheric

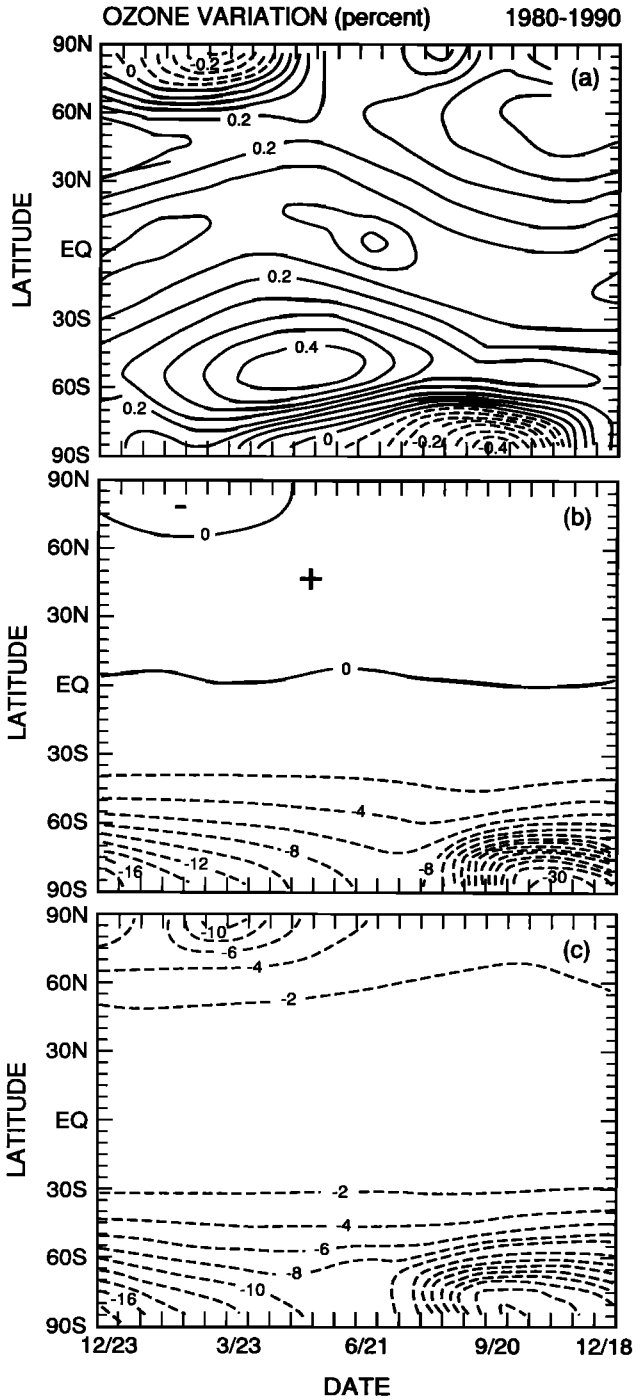

Fig. 18. Relative variation (percent) in the ozone column abundance between 1980 and 1990, shown as a function of latitude and season. (*a*) Heterogeneous processes are ignored, (*b*) heterogeneous processes on the surface of particles in polar stratospheric clouds are taken into account, and (*c*) heterogeneous chemistry in polar stratospheric clouds and on the surface of sulfate aerosol particles is included in the model calculation.

chlorine load increases. Even with limitations of the CFCs emissions resulting from the Montreal Protocol (1987) and subsequent London Revisions (1990), heterogeneous reactions on sulfate aerosols could produce in the next decades a significant ozone depletion, especially after volcanic eruptions such as that of Mount Pinatubo. In addition, if the growth in the large aerosol particles observed by *Hofmann*

TABLE 3. Trend Derived from TOMS Total Ozone Data for the Period November 1978–March 1991 [*Stolarski et al.*, 1992] Compared With Trend Calculated by the Model for the 1980–1990 Period

	TOMS		Model	
Latitude	February	October	February	October
80°N	no data	no data	-8	-3
60°N	-7	-6	-3.5	-2
30°N	-5	-1.5	-1.5	-1.5
0°	-0.5	0	-0.5	-0.5
30°S	-3	-2	-2	-2
60°S	-5	-12	-8	-15
80°S	-12	-40	-14	-30

Values are expressed in percent.

[1990] is confirmed, a future decrease of the ozone concentration could be larger than the one expected from the future increase in the concentration of chlorine species. It is therefore important that future trends in the background aerosol size distribution be monitored, especially in relation to the potential development of a stratospheric aircraft fleet, which should increase the level of the background stratospheric aerosol load in the lower stratosphere.

Because large volcanic eruptions are sporadic and take place at random latitudes, no average representative distributions of the aerosol surface area can be defined for volcanic periods. Idealized volcanic distributions of the aerosol surface density area have, however, been constructed to account for the large perturbations following the eruption of El Chichón (March 1982) in Mexico and Mount Pinatubo in the Philippines (June 1991). The model predicts, at the end of the winter following the eruption of Mount Pinatubo, reductions in the ozone column abundance at high latitudes which could be of the same order as those observed over Antarctica in early spring. The accuracy of such calculations depends on the assumption made for the volcanic clouds after large-scale dispersion and for the efficiency of heterogeneous conversions on the surface of sulfate aerosols. More work is needed to better define and quantify heterogeneous processes.

Acknowledgments. We thank Margaret Tolbert who provided values of reaction probabilities for heterogeneous reactions on aerosol particles and John Gille, who supplied the NO_2 and HNO_3 LIMS data. Helpful discussions with Alan Fried, Rolando Garcia, Sasha Madronich, Stacy Walters, John Orlando, and Susan Solomon are gratefully acknowledged. Claire Granier is supported in part by the Commission of The European Communities (STEP Program) and by the Gas Research Institute (contract 5090-254-1993). Guy Brasseur is supported in part at the University of Brussels by the Global Change Program of the Belgian government. The National Center for Atmospheric Research is sponsored by the National Science Foundation.

REFERENCES

Anderson, J. G., W. H. Brune, and M. H. Profit, Ozone destruction by chlorine radicals within the Antarctic vortex: The spatial and temporal evolution of ClO-O_3 anticorrelation based on in situ ER-2 data, *J. Geophys. Res.*, *94*, 11,465–11,479, 1989.

Andrews, D. G., and M. E. McIntyre, Planetary waves in horizontal and vertical shear: The generalized Eliassen-Palm relation and the mean zonal acceleration, *J. Atmos. Sci.*, *33*, 2031–2048, 1976.

Bais, A. F, C. S. Zerefos, I. C. Ziomas, N. Zoumakis, H. T. Mantis, D. J. Hofmann, and G. Fiocco, Decreases in the ozone and the SO_2 columns following the appearance of the El Chichón aerosol cloud at mid-latitude, in *Atmospheric Ozone, Proceedings of the Quadrennial Ozone Symposium, Halkidiki, Greece*, pp. 352–356, D. Reidel, Hingham, Mass., 1985.

Bekki, S., and J. A. Pyle, Potential impact of the volcanic eruption of Mount Pinatubo on stratospheric aerosol and ozone through heterogeneous chemistry, *Nature*, in press, 1992.

Bernard, A., D. Demaiffe, N. Matielli, R. S. Punong-bayan, Anhydrite-

bearing pumices from Mount Pinatubo: Further evidence for the existence of sulphur-rich silicic magmas, *Nature, 354*, 139–141, 1991.

Boville, B. A., J. R. Holton, and P. W. Mote, Simulation of the Pinatubo aerosol cloud in general circulation model, *Geophys. Res. Lett., 18*, 2281–2284, 1991.

Brasseur, G., Ozone depletion: A deepening, broadening trend, *Nature, 352*, 668–669, 1991.

Brasseur, G., and M. H. Hitchman, The effect of breaking gravity waves on the distribution of trace species in the middle atmosphere, in *Transport Processes in the Middle Atmosphere*, edited by G. Visconti and R. Garcia, pp. 215–227; NATO ASI Series, D. Reidel, Hingham, Mass., 1987.

Brasseur, G., and P. C. Simon, Stratospheric chemical and thermal response to long-term variability in solar UV irradiance, *J. Geophys. Res., 86*, 7343–7362, 1981.

Brasseur, G., and S. Solomon (Eds.), *Aeronomy of the Middle Atmosphere*, D. Reidel, Hingham, Mass., 1986.

Brasseur, G., M. H. Hitchman, S. Walters, M. Dymek, E. Falise, and M. Pirre, An interactive chemical dynamical radiative two-dimensional model of the middle atmosphere, *J. Geophys. Res., 95*, 5639–5655, 1990*a*.

Brasseur, G., C. Granier, and S. Walters, Future changes in stratospheric ozone and the role of heterogeneous chemistry, *Nature, 348*, 626–628, 1990*b*.

Brune, W. H., and J. G. Anderson, In situ observations of ClO in the Antarctic: ER-2 aircraft results from 54°S to 72°S latitude, *J. Geophys. Res., 94*, 16,649–16,663, 1989*a*.

Brune, W. H., and J. G. Anderson, In situ observations of BrO in the Antarctic: ER-2 aircraft results from 54°S to 72°S latitude, *J. Geophys. Res., 94*, 16,639–16,647, 1989*b*.

Cadle, R. D., P. Crutzen, and D. Ehhalt, Heterogeneous chemical reactions in the stratosphere, *J. Geophys. Res., 80*, 3381–3385, 1975.

Chandra, S., and R. S. Stolarski, Recent trends in stratospheric total ozone: Implications of dynamical and El Chichón perturbations, *Geophys. Res. Lett., 18*, 2277–2280, 1991.

Considine, D. B., A. R. Douglass, and R. Stolarski, Heterogeneous conversion of N_2O_5 to HNO_3 on background stratospheric aerosols: Comparisons of model results with data, *Geophys. Res. Lett., 19*, 397–400, 1992.

Crutzen, P. J., The possible importance of CSO for the sulfate layer of the stratosphere, *Geophys. Res. Lett., 3*, 73–76, 1976.

DeMore, W. B., S. P. Sander, D. M. Golden, M. J. Molina, R. F. Hampson, M. J. Kurylo, C. J. Howard, and A. R. Ravishankara, Chemical kinetics and photochemical data for use in stratospheric modeling, Evaluation Number 9, *JPL Publ. 90-1*, Jet Propulsion Lab., Pasadena, Calif., 1990.

Dütsch, H. U., Total ozone trend in the light of ozone soundings, the impact of El Chichón, in *Atmospheric Ozone, Proceedings of the Quadrennial Ozone Symposium, Halkidiki, Greece*, pp. 263–268, D. Reidel, Hingham, Mass., 1985.

Fried, A., B. Henry, J. G. Calvert, and M. Mozurkewich, Reaction probabilities of N_2O_5 on submicrometer H_2SO_4 aerosols under stratospheric conditions, AGU Spring Meeting, Invited paper number A42B-F, May 28–31, 1991, Baltimore, Maryland.

Gardiner, B. G., Comparative morphology of the vertical ozone profile in the Antarctic spring, *Geophys. Res. Lett., 15*, 901–904, 1988.

Hanson, D. H., and A. R. Ravishankara, The reaction probability of $ClONO_2$ and N_2O_5 on 40 to 75% sulfuric acid solutions, *J. Geophys. Res., 96*, 17,307–17,314, 1991.

Hitchman, M. H., and G. Brasseur, Rossby wave activity in a two-dimensional model: Closure for wave driving and meridional eddy diffusivity, *J. Geophys. Res., 93*, 9405–9417, 1988.

Hofmann, D. J., Perturbations to the global atmosphere associated with the El Chichón volcanic eruption of 1982, *Rev. Geophys., 25*, 743–759, 1987.

Hofmann, D. J., Increase in the stratospheric background sulfuric acid aerosol mass in the past 10 years, *Science, 248*, 996–1000, 1990.

Hofmann, D. J., and J. M. Rosen, Measurement of the sulfuric acid weight percent in the stratospheric aerosol from the El Chichón eruption, *Geofis. Int., 23-3*, 309–320, 1984*a*.

Hofmann, D. J., and J. M. Rosen, On the temporal variation of stratospheric aerosol size and mass during the first 18 months following the 1982 eruptions of El Chichón, *J. Geophys. Res., 89*, 4883–4890, 1984*b*.

Hofmann, D. J., and S. Solomon, Ozone destruction through heterogeneous chemistry following the eruption of El Chichón, *J. Geophys. Res., 94*, 5029–5041, 1989.

Hofmann, D. J., J. M. Rosen, and J. W. Harder, Aerosol measurements in the winter/spring Antarctic stratosphere, 1, Correlative measurements with ozone, *J. Geophys. Res., 93*, 665–676, 1988.

Hofmann, D. J., J. M. Rosen, J. W. Harder, and J. V. Hereford, Balloon-borne measurements of aerosol, condensation nuclei, and cloud particles in the stratosphere at McMurdo Station, Antarctica, during the spring of 1987, *J. Geophys. Res., 94*, 11,253–11,269, 1989.

Junge, C. E., C. W. Chagnon, and J. E. Manson, Stratospheric aerosols, *J. Meteorol., 18*, 81–108, 1961.

Kiehl, J. T., R. J. Wolski, B. P. Briegleb, and V. Ramanathan, Documentation of radiation and cloud routines in the NCAR Community Climate Model (CCM1), *NCAR Tech. Note, NCAR/TN-288+IA*, Natl. Cent. for Atmos. Res., Boulder, Colo., 1987.

Komhyr, W. D., S. J. Oltmans, and R. D. Grass, Atmospheric ozone at south pole, Antarctica in 1986, *J. Geophys. Res., 93*, 5167–5184, 1988.

Leu, M. T., Laboratory studies of sticking coefficients and heterogeneous reactions important in the Antarctic stratosphere, *Geophys. Res. Lett., 15*, 17–20, 1988.

Mantis, H. T., C. S. Zerefos, A. Bais, I. Ziomas, and A. Kelessis, The northern hemisphere ozone minimum in 1982-1983, *Arch. Meteorol. Geophys. Bioclimatol., Ser. B, 36*, 135–145, 1986.

McCormick, M. P., and R. E. Veiga, SAGE II measurements of early Pinatubo aerosols, *Geophys. Res. Lett., 19*, 155–158, 1992.

McCormick, M. P., P. Hamill, J. J. Pepin, W. P. Chu, T. J. Swissler, and L. R. McMaster, Satellite studies of the stratospheric aerosol, *Bull. Am. Meteorol. Soc., 60*, 1038–1046, 1979.

McCormick, M. P., H. M. Steele, P. Hamill, W. P. Chu, and T. J. Swissler, Polar stratospheric cloud sightings by SAM II, *J. Atmos. Sci., 39*, 1387–1397, 1982.

McCormick, M. P., T. J. Swissler, W. H. Fuller, W. H. Hunt, and M. T. Osborn, Airborne and ground-based lidar measurements of the El Chichón stratospheric aerosol from 90°N to 90°S, *Geofis. Int., 23*, 187–221, 1984.

McCormick, M. P., C. R. Trepte, and M. C. Pitts, Persistence of polar stratospheric clouds in the southern polar region, *J. Geophys. Res., 94*, 11,241–11,251, 1989.

McElroy, M. B., R. J. Salawitch, S. C. Wofsy, and J. A. Logan, Reductions of Antarctic ozone due to synergistic interactions of chlorine and bromine, *Nature, 321*, 759–762, 1986.

Molina, L. T., and M. J. Molina, Production of Cl_2O_2 from the self-reaction of the ClO radical, *J. Phys. Chem., 91*, 433–436, 1987.

Molina, M. J., T. L. Tso, L. T. Molina, and F. C. Y. Wang, Antarctic stratospheric chemistry of chlorine nitrate, hydrogen chloride, and ice: Release of active chlorine, *Science, 238*, 1253–1257, 1987.

Mozurkewich, M., and J. G. Calvert, Reaction probabilities of N_2O_5 on aqueous aerosols, *J. Geophys. Res., 93*, 15,889–15,896, 1988.

Prather, M., Catastrophic loss of stratospheric ozone in dense volcanic clouds, *J. Geophys. Res., 97*, 10,187–10,191, 1992.

Roscoe, H. K., B. J. Kerridge, L. J. Gray, R. J. Wells, and J. A. Pyle, Simultaneous measurements of stratospheric NO and NO_2 and their comparison with model predictions, *J. Geophys. Res., 91*, 5405–5419, 1986.

Rosen, J. M., The boiling point of stratospheric aerosols, *J. Atmos. Meteorol., 10*, 1044–1045, 1971.

Rosen, J. M., D. J. Hofmann, and J. Laby, Stratospheric aerosol measurements II: Worldwide distribution, *J. Atmos. Sci., 32*, 1457–1462, 1975.

Simon, P. C., D. Gillotay, N. Vanlaethem-Meuree, and J. Wisemberg, Ultraviolet absorption cross-sections of chloro- and chlorofluoromethanes at stratospheric temperatures, *J. Atmos. Chem., 7*, 107–135, 1988.

Solomon, S., R. Garcia, F. S. Rowland, and D. Wuebbles, On the depletion of Antarctic ozone, *Nature, 321*, 755, 1986.

Steele, H. M., and P. Hamill, Effects of temperature and humidity on the growth and optical properties of sulphuric acid-water droplets in the stratosphere, *J. Aerosol Sci., 12*, 517–528, 1981.

Stolarski, R. S., P. Bloomfield, R. D. McPeters, and J. R. Herman, Total ozone trends deduced from Nimbus 7 TOMS data, *Geophys. Res. Lett., 18*, 1015–1018, 1991.

Stolarski, R., R. Bojkov, L. Bishop, C. Zerefos, J. Stachelin, and J. Zawodny, Measured trends in stratospheric ozone, *Science, 256*, 342–349, 1992.

Tolbert, M. A., M. J. Rossi, and D. M. Golden, Heterogeneous interactions of chlorine nitrate, hydrogen chloride, and nitric acid with sulfuric acid surfaces at stratospheric temperatures, *Geophys. Res. Lett., 15*, 847–850, 1988*a*.

Tolbert, M. A., M. J. Rossi, and D. M. Golden, Antarctic ozone depletion chemistry : reactions of N_2O_5 with H_2O and HCl on ice surfaces, *Science, 240*, 1018–1021, 1988*b*.

Toon, O. W., R. P. Turco, J. Jordan, J. Goodman, and G. Ferry, Physical processes in polar stratospheric ice clouds, *J. Geophys. Res., 94*, 11,359–11,380, 1989.

Turco, R. P., P. Hamill, O. B. Toon, R. C. Whitten, and C. S. Kiang, A one-dimensional model describing aerosol formation and evolution in the stratosphere, I, Physical processes and mathematical analogs, *J. Atmos. Sci., 36*, 699–717, 1979.

Turco, R. P., R. C. Whitten, and O. B. Toon, Stratospheric aerosols: Observation and theory, *Rev. Geophys., 20*, 233–279, 1982.

Turco, R. P., O. B. Toon, and P. Hamill, Heterogeneous physicochemistry of the polar ozone hole, *J. Geophys. Res., 94*, 16,493–16,510, 1989.

World Meteorological Organization, *Scientific Assessment of Stratospheric Ozone: 1989, Global Ozone Research and Monitoring Project*, Geneva, 1990.

World Meteorological Organization, *Scientific Assessment of Ozone Depletion: 1991, Global Ozone Research and Monitoring Project*, Geneva, in press, 1992.

Worsnop, D. M., M. Zahniser, C. Kolb, L. Watson, J. Van Doren, J. Jayne, and P. Davidovits, Mass accommodation coefficient measurements for HNO_3, HCl and N_2O_5 on water, ice and aqueous sulfuric acid droplet surfaces, Polar Ozone Workshop, National Aeronautics and Space Administration, Snowmass, Colo., May 1988.

G. Brasseur and Claire Granier, National Center for Atmospheric Research, P. O. Box 3000, Boulder, CO 80307.

(Received March 26, 1992;
revised August 21, 1992;
accepted August 25, 1992.)